



الجمهورية الجزائرية الديمقراطية الشعبية
People's Democratic Republic of Algeria

وزارة التعليم العالي والبحث العلمي
Ministry of Higher Education and Scientific Research

جامعة غرداية
University of Ghardaia

Registration n°:
...../...../...../...../.....

والتكنولوجيا العلوم كلية
Faculty of Science and Technology

قسم الرياضيات والإعلام الآلي
Department of Mathematics and Computer Science

التطبيقية والعلوم الرياضيات مخبر
Mathematics and Applied Sciences Laboratory

A Thesis Submitted in Partial Fulfillment of the Requirements for the Degree of

Master

Domain: Mathematics and Computer Science

Field: Computer Science

Specialty: Intelligent Systems for Knowledge Extraction

Topic

Alzheimer's Disease Detection using Deep Learning Techniques

Presented by:

Brahim AISSA & Nacer BENYOUB

Publicly defended on September 22, 2024

Jury members:

MR. SLIMANE OULAD-NAOUI	MCB	Univ. Ghardaia	President
MR. ABDERRHAMANE ADJILA	MAA	Univ. Ghardaia	Examiner
MR. ATTIA NEHAR	MCA	Univ. Z.A. Djelfa	Supervisor
MR. SLIMANE BELLAOUAR	MCA	Univ. Ghardaia	Co-Supervisor

Academic Year: 2023/2024

Acknowledgment

We thank Allah for giving us the guidance, patience, and health to be able to carry out this graduation project.

We also thank all the members of our families for their support. We extend our deepest gratitude to all our teachers of the Computer Science department in the university of Ghardaia. Especially, Mr Attia Nehar and Mr Slimane Bellaouar for their huge efforts in supervising and guiding us.

Dedication

To my mother, and family who show me continued and unconditional encouragement, love, and prayer.

To my friends and colleagues, who offered me their precious time and support.

Dedication

To my beloved parents, thank you for your sacrifices, support, and endless encouragement throughout this journey.

To my dear family, for your patience, unwavering belief in me, and constant words of encouragement that have motivated me to persevere.

To my colleagues and friends, for their unwavering companionship and understanding during the challenging moments.

To my mentors, who shared this journey with me, and whose guidance played a crucial role in completing this work.

Thank you all, from the bottom of my heart.

ملخص

مرض الزهايمر (DA) هو اضطراب تنكسي عصبي تدريجي لا يملك علاجاً فعالاً. كونه السبب الأكثر شيوعاً للخرف، فإنه يؤثر على ملايين الأشخاص حول العالم، مما يجعل الاكتشاف المبكر والتشخيص ضرورة. يمكن للتعلم العميق أن يساعد في اكتشاف الأنماط العديدة المرتبطة بهذا المرض، مما يسهم في تشخيصه المبكر. في هذا العمل، نستخدم طريقة تعلم النقل التحويلي لتصنيف صور الرنين المغناطيسي إلى فئات مرض الزهايمر (DA) والضعف الإدراكي البسيط (ICM) والأشخاص السليمين إدراكياً (NC) من خلال استخدام نموذج 61GGV و 91GGV التي تم تدريبها مسبقاً على مجموعة بيانات teNegamI. تم استخدام مجموعات بيانات تم تقليل حجمها وزيادته مأخوذة من مجموعة بيانات INDA للتخفيف من مشكلة عدم توازن الفئات، مما أدى إلى إجراء أربع تجارب. أسفرت نهجنا عن معدلات دقة عالية تتراوح من 89%.41 إلى 99%.95، حيث حقق نموذج 91GGV المدرب على البيانات المحفظة الحجم أعلى أداء بين النماذج الأربعة.

كلمات مفتاحية: مرض الزهايمر، التعلم العميق، تعلم النقل التحويلي، الخرف، الشبكات العصبية الالتفافية، GGV، التصوير بالرنين المغناطيسي.

Abstract

Alzheimer's Disease (AD) is a progressive and irreversible neurodegenerative disorder. Being the most common cause of dementia, it affects millions of people around the world, making early detection and diagnosis a necessity. Deep learning can help detect the numerous patterns associated with this disease, aiding in its early diagnosis. In this work, we employ a transfer learning approach to classify MRI images into Alzheimer's Disease (AD), Mild Cognitive Impairment (MCI), and Cognitively Normal (CN) classes by leveraging VGG16 and VGG19 models pre-trained on ImageNet. The datasets used for training are down-sampled and up-sampled datasets sampled from the ADNI dataset to mitigate the class imbalance issue, resulting in four experiments. Our approach yielded high accuracy rates ranging from 98.14% to 99.59%, with VGG19 trained on down-sampled data achieving the highest performance among the four models.

Keywords: Alzheimer's Disease, Deep learning, Transfer learning, Dementia, Convolutional Neural Networks, VGG, MRI.

Résumé

La maladie d'Alzheimer (AD) est un trouble neurodégénératif progressif et irréversible. Étant la cause la plus courante de démence, elle affecte des millions de personnes dans le monde, rendant la détection et le diagnostic précoces essentiels. L'apprentissage profond peut aider à détecter les nombreux motifs associés à cette maladie, facilitant ainsi son diagnostic précoce. Dans ce travail, nous employons une approche d'apprentissage par transfert pour classer les images IRM en trois catégories : maladie d'Alzheimer (AD), déficit cognitif léger (MCI) et personnes cognitivement normales (CN), en utilisant les modèles VGG16 et VGG19 pré-entraînés sur ImageNet. Les ensembles de données utilisés pour l'entraînement sont des ensembles réduits et augmentés, échantillonnés à partir de la base de données ADNI pour atténuer le problème de déséquilibre des classes, aboutissant à quatre expériences. Notre approche a donné des taux de précision élevés allant de 98,14% à 99,59%, le modèle VGG19 entraîné sur les données réduites ayant obtenu les meilleures performances parmi les quatre modèles.

Mots clés: La maladie d'Alzheimer, Apprentissage profond, Apprentissage par transfert, démence, réseaux neuronaux convolutifs, VGG, IRM.

Contents

List of Figures	x
List of Tables	xi
List of Acronyms	xi
Introduction	1
1 Basic Concepts	2
1.1 Alzheimer Disease	2
1.2 Neuroimaging	3
1.3 Imaging Modalities	3
1.3.1 Computerized Tomography (CT)	3
1.3.2 Positron Emission Tomography (PET)	4
1.3.3 Fluorodeoxyglucose Positron Emission Tomography	5
1.3.4 SPECT images	5
1.3.5 Magnetic Resonance Imaging (MRI): sMRI, fMRI	6
1.3.6 Diffusion Tensor (DTI)	7
1.4 Deep learning	7
1.4.1 Introduction	7
1.4.2 Deep Learning Architectures	9
1.4.3 VGG Architecture	10
2 State Of The Art	11
2.1 Introduction	11
2.2 Classic Approaches	11
2.3 Machine Learning-based Approaches	12

2.3.1	Bayesian Classifier	12
2.3.2	Support Vector Machines	12
2.3.3	Logistic Regression	13
2.3.4	K-means	14
2.3.5	Multi-layer Perceptron	15
2.4	Deep Learning-based Approaches	15
2.4.1	Transfer Learning (TL) approaches	15
2.4.2	Convolutional Neural Networks	16
2.4.3	Recurrent Neural Networks	17
2.4.4	Generative Adversarial Networks	17
2.4.5	Transformer-Based Approaches	18
2.5	Conclusion	19
3	Implementation and Experiments	22
3.1	Introduction	22
3.2	Data	22
3.3	Preprocessing	23
3.4	Experiments	24
3.4.1	Architecture	24
3.4.2	Metrics Used in Evaluation	24
3.4.3	Experimental results	25
3.4.3.1	Training on down-sampled data	26
3.4.3.2	Training on up-sampled data	26
3.4.4	Discussion	30
3.5	Conclusion	33
	Conclusion and Perspectives	35
	References	36
	Appendices	40
A	Deposit Permission	41

List of Figures

1.1	An example of a CT scan	4
1.2	An example of a PET scan	5
1.3	An example of an PET-FDG scan	6
1.4	An example of a SPECT scan	7
1.5	An example of an MRI scan	8
1.6	An example of an DTI scan	8
1.7	VGG 16 Architecture	10
3.1	Training and validation loss of VGG16 trained on down-sampled data	27
3.2	Confusion matrix of VGG16 trained on down-sampled data	27
3.3	Receiver Operating Characteristic curve of VGG16 trained on down-sampled data	27
3.4	Training and validation loss of VGG19 trained on down-sampled data	28
3.5	Confusion matrix of VGG19 trained on down-sampled data	28
3.6	Receiver Operating Characteristic curve of VGG19 trained on down-sampled data	28
3.7	Training and validation loss of VGG16 model trained on up-sampled data	29
3.8	Confusion Matrix of VGG16 on up-sampled data	29
3.9	Receiver Operating Characteristic curve of VGG16 trained on up-sampled data	29
3.10	Training and validation loss of VGG19 trained on up-sampled data	31
3.11	Confusion matrix of VGG19 trained on up-sampled data	31
3.12	Receiver Operating Characteristic curve of VGG19 trained on up-sampled data	31
3.13	Comparison of models performance across all metrics	33
3.14	Comparison of model's recall by class.	33

3.15 Comparison of models F1-score by class	33
---	----

List of Tables

2.1	Recapitulating table of machine learning contributions to AD classification	20
2.2	Recapitulating table of deep learning contributions to AD classification	21
3.1	Classification Report of VGG16 trained on down-sampled data . . .	26
3.2	Classification Report of VGG19 trained on down-sampled data . . .	26
3.3	Classification Report of VGG16 trained on up-sampled data	30
3.4	Classification Report of VGG19 trained on up-sampled data	30
3.5	Model Performance Summary.	32
3.6	Comparison of the recent studies with proposed approach	32

Introduction

According to the World Health Organization (WHO)¹, the number of people with dementia worldwide is expected to rise from 55 million in 2019 to 139 million by 2050. The economic burden of dementia is projected to increase significantly, from US\$ 1.3 trillion annually in 2019 to an estimated \$2.8 trillion by 2030. Alzheimer’s Disease (AD), the most common cause of dementia, currently has no effective treatment to stop or reverse its progression, though treatments exist to improve symptoms (Kumar et al. (2023)).

Diagnosing AD is challenging due to the brain’s complexity and the potential confusion with other diseases. Additionally, AD symptoms typically do not manifest in the early stages. This underscores the critical need for early detection to anticipate and prevent the progression of AD, ensuring that affected individuals and their caregivers enjoy a better quality of life. To this end, various deep learning techniques have been explored for early detection and recognition of AD stages using modalities such as imaging, clinical tests, and genetic data to assist physicians in diagnosis. These techniques include Convolutional Neural Networks (CNN) (Raju et al. (2021), Ebrahimi et al. (2021)), Recurrent Neural Networks (RNN) (Wang et al. (2018) and Aqeel et al. (2022)), Transfer Learning, as in Hon & Khan (2017) and Aderghal et al. (2018), and generative models (S. Saravanakumar (2022) and Sampath et al. (2023)), among others. While these approaches have shown promising results, the need for larger labeled datasets that offer class balance is constantly present, especially in specialized fields.

In this work, we employ transfer learning techniques to classify MRI images into three categories: Alzheimer’s Disease (AD), Mild Cognitive Impairment (MCI), and Cognitively Normal (CN). We leverage the VGG16 and VGG19 models from the VGG architecture (Simonyan & Zisserman (2015)), pre-trained on ImageNet. To address class imbalance, we train on both down-sampled and up-sampled datasets extracted from the ADNI dataset.

The rest of this thesis is organized as follows. Chapter 1 is devoted to the definition of concepts that are essential for the understanding of this work. In Chapter 2, we review key contributions in machine learning and deep learning for AD research. Chapter 3 details our data collection, preprocessing, and model training processes, and presents and discusses the results. Finally, we conclude by summarizing the addressed problem, the implementation steps, the results, the limitations, and the future perspectives.

¹<https://www.who.int/news-room/facts-in-pictures/detail/dementia>

Chapter 1

Basic Concepts

1.1 Alzheimer Disease

In 1901, Dr. Alois Alzheimer, a German psychiatrist with expertise in neuropathology, treated a 51-year-old patient named Auguste Deter, who exhibited symptoms of memory loss, psychological changes, and disorientation. After she died in 1906, Alzheimer performed an autopsy and he discovered two brain abnormalities: plaques and tangles, which are now known as beta-amyloid plaques and tau tangles. This marked the beginning of our understanding of Alzheimer's Disease as a brain disorder that required medical treatment. Alzheimer's Disease (AD) is a progressive neurodegenerative disorder that affects the brain, leading to cognitive decline, memory loss, and changes in behavior and personality. It is the most common cause of dementia, affecting millions of people around the world.

Alzheimer's disease progresses from subtle cognitive changes to severe stages in memory loss, thinking, and the ability to perform daily activities. Typically, Alzheimer's progresses gradually, starting with preclinical (no noticeable symptoms, but brain changes start to occur). The next stage is mild cognitive impairment (MCI) with slight memory problems. The middle stage (Moderate Alzheimer's Disease) comes with symptoms such as cognitive decline and behavioral changes. The late stage (Severe Alzheimer's Disease) is characterized by severe cognitive and physical deterioration that requires full-time care. It is important to note that it can be challenging to assign a person with Alzheimer's to a specific stage, as symptoms and progression often overlap. Diagnosing Alzheimer's Disease and then treating it is not easy. Generally, early diagnosis is more straightforward when treating the disease in the advanced stages. Early diagnosis of Alzheimer's allows for timely medical intervention to slow the progression of symptoms, which can contribute to a longer life. It informs individuals and their families to make decisions about future care and living arrangements, like engaging in mental and physical activities, to improve the life quality for both patients and caregivers. Also, early diagnosis of patients provides the opportunity to treat using clinical trials. However, Diagnosing Alzheimer's is still challenging due to the overlap with normal aging symptoms, such as mild memory loss, stress, and depression. Additionally, some comorbidities, such as thyroid issues, can mask or mimic Alzheimer's symptoms, making it difficult to distinguish between them, especially with a lack of a single definitive test. In addition, Stigma and denial often surrounding AD diagnosis can significantly delay

proper treatment and support.

1.2 Neuroimaging

Neuroimaging is a branch of medical imaging that specifically focuses on the brain. As a clinical specialty, it employs non-invasive techniques to produce detailed images. These images are used then for visualizing the structure and function of the brain, It is necessary for diagnosing and studying gross injury and intracranial diseases such as Alzheimer's disease. Neuroimaging has various modalities including MRI, PET, SPECT, and others, each modality addresses specific diagnostic needs due to the brain's complexity, and their combination usage provides unique perspectives and insights to understanding a patient's condition.

1.3 Imaging Modalities

Medical Diagnosis often requires information beyond what physical examination can offer. Image modalities act as windows into the human body, providing various techniques to visualize the body and its internal structures and functions. These techniques employ different technologies and physical principles and provide detailed images of anatomical structures and physiological functions. The variety of image modalities allows doctors and professionals to choose appropriate methods for specific diagnostic needs, and each technique shows different distinct advantages and insights. Some modalities capture detailed anatomical structures, while others are better suited for visualizing functional or tracking brain activity. The complexity of human anatomy and physiology makes it difficult to provide all the necessary information with a single imaging technique for a comprehensive diagnosis. Multiple modalities can make more accurate diagnoses and develop more effective treatment plans. We will explore several imaging modalities that are used in diagnostic Alzheimer's disease, including Computed Tomography (CT), Positron Emission Tomography (PET), and Magnetic Resonance Imaging (MRI), highlighting their specific uses, benefits, and the dataset and their advantages and disadvantages.

1.3.1 Computerized Tomography (CT)

Computed Tomography (CT) is a diagnostic imaging technique that uses X-ray technology to produce detailed cross-sectional images of the body, including the bones, organs, and blood vessels. It combines X-rays taken from different angles with computer processing to create these images, which provide more detailed information than standard X-rays. CT scans can be used to identify diseases, injuries, and other medical conditions in various parts of the body, making them valuable for diagnosis, treatment planning, and screening purposes.

The benefits of CT scans include their ability to provide detailed information for diagnosing and planning treatment for a wide range of medical conditions. They are particularly well-suited for quickly examining people who may have internal injuries

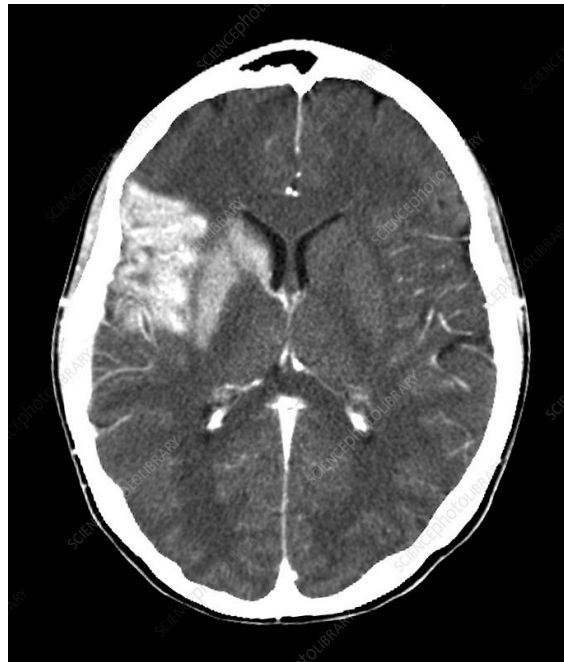


Figure 1.1: An example of a CT scan

from accidents or trauma. CT scans can also be used for fluid or tissue biopsies or as part of preparation for surgery or treatment. However, there are some risks associated with CT scans. The primary concern is exposure to ionizing radiation, which may cause a small increase in a person's lifetime risk of developing cancer. Additionally, there is a possible risk of reaction to the intravenous contrast agent or dye, which is used to improve visualization in some CT scans. Despite these risks, when used appropriately, the benefits of a CT scan far exceed the risks.

1.3.2 Positron Emission Tomography (PET)

Positron Emission Tomography (PET) is a medical imaging technique that uses a radioactive tracer to visualize metabolic activity in the body. PET scans are used to diagnose and monitor various medical conditions, including cancer, heart disease, and neurological disorders. PET imaging is increasingly being used in machine learning and deep learning applications. The benefits of PET imaging include its ability to detect metabolic changes in the body, which can help diagnose and monitor medical conditions. However, PET imaging also carries some risks, including exposure to radiation and potential allergic reactions to the tracer. There are several open datasets available for use in machine learning and deep learning applications, including the Alzheimer's Disease Neuroimaging Initiative (ADNI) dataset ¹, which includes PET scans of patients with Alzheimer's Disease.

¹Official website: adni.loni.usc.edu

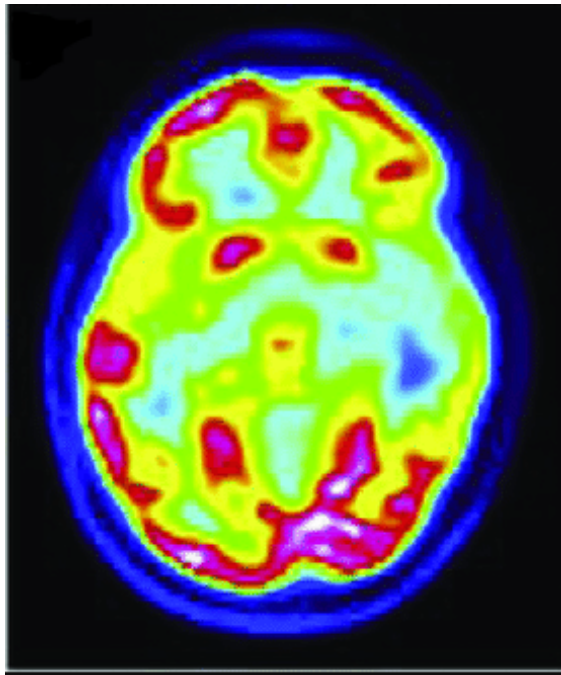


Figure 1.2: An example of a PET scan

1.3.3 Fluorodeoxyglucose Positron Emission Tomography

FDG-PET stands for [F18] Fluorodeoxyglucose Positron Emission Tomography. It is a medical imaging technique that combines positron emission tomography (PET) with a radioactive glucose tracer called fluorodeoxyglucose (FDG) to highlight metabolic activity in the body, including the brain. FDG is a radioactive form of glucose, a type of sugar that cells in the body use for energy. FDG-PET is commonly used in oncology to detect and locate tumors, evaluate the extent of disease, and assess treatment response, Nabi & Zubeldia (2002). In the context of Alzheimer's Disease detection, FDG-PET plays a crucial role by capturing patterns of glucose uptake, revealing areas of altered metabolism associated with the disease. In this diagnostic approach, FDG-PET data is integrated with machine learning algorithms, deep learning models in particular, to analyze and interpret subtle changes in glucose metabolism patterns. It's important to note that while these approaches show promise, the interpretation of FDG-PET findings in Alzheimer's Disease remains complex, and integration with other diagnostic tools is often necessary. Drawbacks include exposure to ionizing radiation, cost considerations, and potential interpretational challenges. In addition, these models are research tools and should be used in conjunction with clinical experience.

1.3.4 SPECT images

Single-photon emission computed tomography (SPECT) is a nuclear medicine imaging technique that provides three-dimensional information about the distribution of radioactive tracers in a patient's body. The process begins with the injection of a small amount of radioactive tracer into the patient. As the radiotracer circulates through the body, it accumulates in the target tissues. A gamma camera then rotates around the patient, detecting the radiotracer's distribution and creating de-

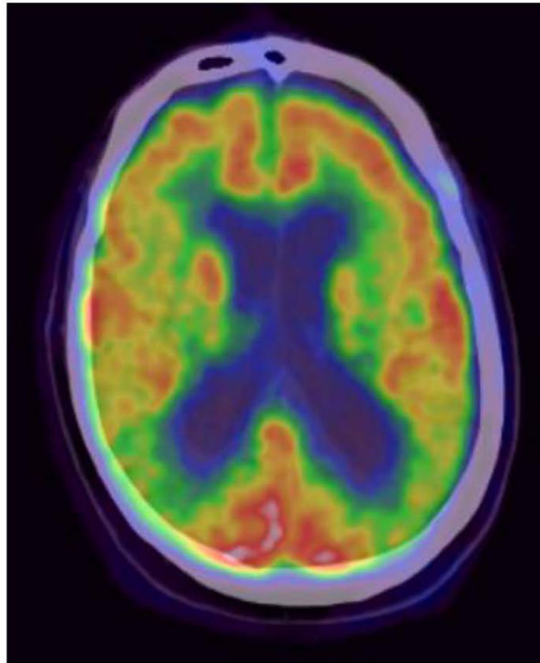


Figure 1.3: An example of an PET-FDG scan

tailed images of organs, bones, and tissues. This imaging technique offers clinicians valuable insights into the perfusion and functionality of specific tissues, helping to identify variations in brain activity associated with Alzheimer’s disease and other neurological disorders. The radioactive tracer generally does not cause side effects and typically leaves the body within 24 hours. Although SPECT is considered safe, there are potential side effects, such as bleeding, pain, swelling at the injection site, and allergic reactions to the tracer, particularly in patients with pre-existing conditions or allergies. Healthcare providers must carefully manage the radiation dosage. The use of SPECT imaging in scientific research and clinical studies is supported by various datasets, such as OASIS ² and PPMI. However, these datasets are generally not publicly available.

1.3.5 Magnetic Resonance Imaging (MRI): sMRI, fMRI

Magnetic Resonance Imaging (MRI) is a non-invasive medical imaging technique that uses a strong magnetic field and radio waves to produce detailed two and three-dimensional anatomical images of the body, such as bones, muscles, blood vessels, and the brain. It provides better soft tissue contrast than CT scans and does not use ionizing radiation, making it a safer imaging option. MRI can be used to diagnose a variety of conditions, including anomalies of the brain and spinal cord, tumors, joint injuries, heart problems, and diseases of the liver and other abdominal organs. Specifically, structural MRI (sMRI) offers detailed images of brain anatomy, allowing for the detection of subtle changes like brain atrophy, a hallmark of Alzheimer’s disease. Functional MRI (fMRI) measures brain activity by detecting blood flow changes, providing insights into functional alterations and connectivity patterns in the brain. While MRI carries minimal risks, they may include the need for patients to remain very still during the procedure, the potential for sedation or

²Official website: sites.wustl.edu/oasisbrains

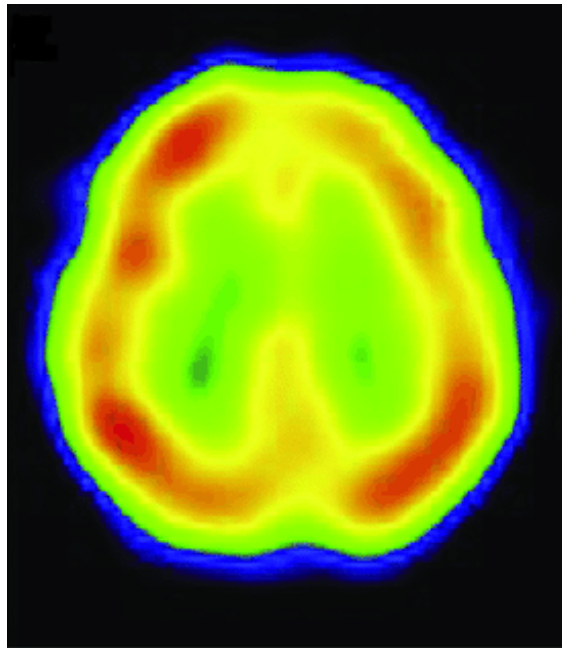


Figure 1.4: An example of a SPECT scan

anesthesia in some cases, and unique safety hazards for patients with implants or external medical devices. Regarding the availability of Alzheimer’s disease (AD) MRI data in open datasets, ADNI and OASIS are commonly used in AD research employing machine learning and deep learning techniques.

1.3.6 Diffusion Tensor (DTI)

Diffusion Tensor Imaging (DTI) is a medical imaging technique that uses magnetic resonance imaging (MRI) to visualize the movement of water molecules in the brain’s white matter tracts. DTI can also be used to track changes in white matter at different points in time, providing new insights into the progression of AD. However, there are some risks associated with DTI, such as the potential for the strong magnetic field to attract magnetic objects and the possibility of claustrophobia for some patients. As for the availability of AD-related DTI data, several publicly available datasets include DTI imaging data for AD research. For example, the AI4AD and ADNI datasets.

1.4 Deep learning

1.4.1 Introduction

Deep learning is a subfield of machine learning that is characterized by using deep artificial neural networks (ANN) that vaguely mimic the human brain. These neural networks consist of interconnected nodes called neurons. Organized in layers, they receive input and apply a series of nonlinear transformations to produce an output to learn complex representations from the data. Another core concept is activation functions, which are functions that determine the outputs of neurons

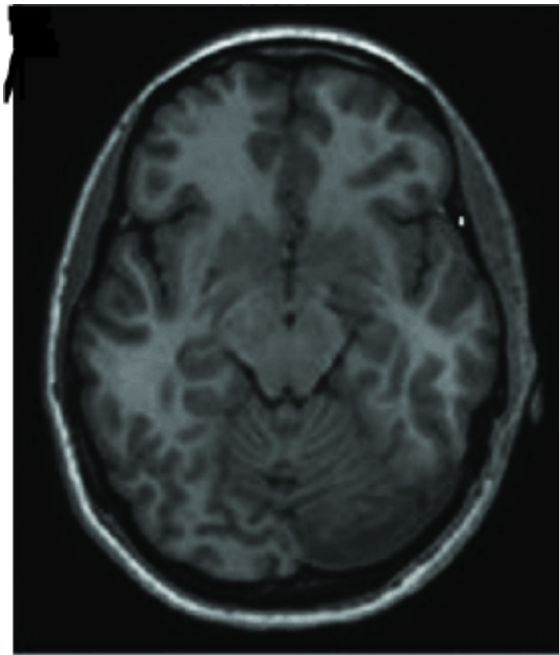


Figure 1.5: An example of an MRI scan

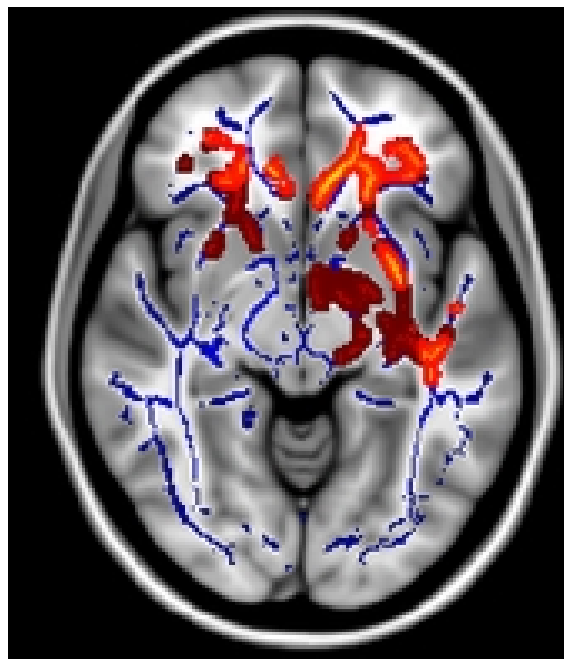


Figure 1.6: An example of an DTI scan

and add non-linearity to the network, which enables it to learn complex patterns from the data.

Deep learning surpasses traditional machine learning in various tasks, particularly complex ones like image labeling, speech recognition, and language translation. This is due to its use of neural networks, which provide multiple layers of abstraction to learn complex relationships in the data [Dubey & Rasool \(n.d.\)](#). Deep learning models automatically extract and learn relevant features without human-led feature engineering, uncovering hidden features and leading to increasing accuracy. Additionally, deep learning's capability to handle and learn from large datasets gives it an edge over traditional methods, especially in the era of big data, where it can

fully leverage its potential Jan et al. (2017). These advantages make deep learning superior to traditional machine learning approaches to complex tasks.

Using deep learning in the healthcare sector has seen increasing interest, as deep learning models have shown significant promise when exploited to perform various health-related tasks such as disease detection, diagnosis, and prediction, as well as classification and tissue segmentation. Deep learning models have also been used to analyze neuroimaging data to diagnose and predict AD due to their ability to handle high-dimensional data such as MRI and PET scans as well as identifying the intricate patterns in the brain and using them to distinguish between the different cases in the data such as CN, MCI, and AD, subsequently achieving high performances.

1.4.2 Deep Learning Architectures

Many neural network architectures have been proposed for deep learning. In addition to ANNs, Convolutional Neural Networks (CNN) and Recurrent Neural Networks (RNN) as well as generative models are among the most widely used architectures. While most of these architectures have been used in AD-related research, each responds to specific types of tasks and challenges.

- **Convolutional Neural Networks (CNNs):** CNNs LeCun et al. (2015) are deep learning architectures that are well suited for image processing tasks. Their main highlight is convolutional layers, which consist of filters that apply to the input image to extract relevant features and patterns through convolution. The weights of these filters are learnable and are updated by an optimization algorithm (typically, a back propagation algorithm LeCun et al. (1989)). CNNs also feature pooling layers, which are layers that downsample the feature maps obtained from convolutional layers, capturing essential representations regardless of their position, orientation, and scale within the image. Typically, the deeper these layers are in the network, the more abstract and high-level the features they capture become. In the context of AD, convolutional and pooling layers allow for the recognition of the various intricate patterns that reflect the changes in the brain, leading to the accurate recognition and classification of the different AD cases and phases, Ebrahimi et al. (2021), Helaly et al. (2021).
- **Recurrent Neural Networks (RNNs):** RNNs are known for being designed to handle sequential data, such as time series and natural language, by introducing recurrent connections that they use to maintain an internal state Minsky & Papert (1988), Rumelhart et al. (1986). This hidden state is updated by processing current input data along with the hidden state from the previous step, which allows context to persist over time. Using this mechanism, these networks are able to model temporal dependencies and capture patterns in sequential data Alsubaie et al. (2024). RNNs have been developed to mitigate some issues with the original architecture, like vanishing gradients. LSTM and GRU are examples of such developments. These architectures have been used in AD research to analyze longitudinal neuroimaging data captured over time and predict AD progression. They were also used to handle multimodality, such as combining neuroimaging with clinical and

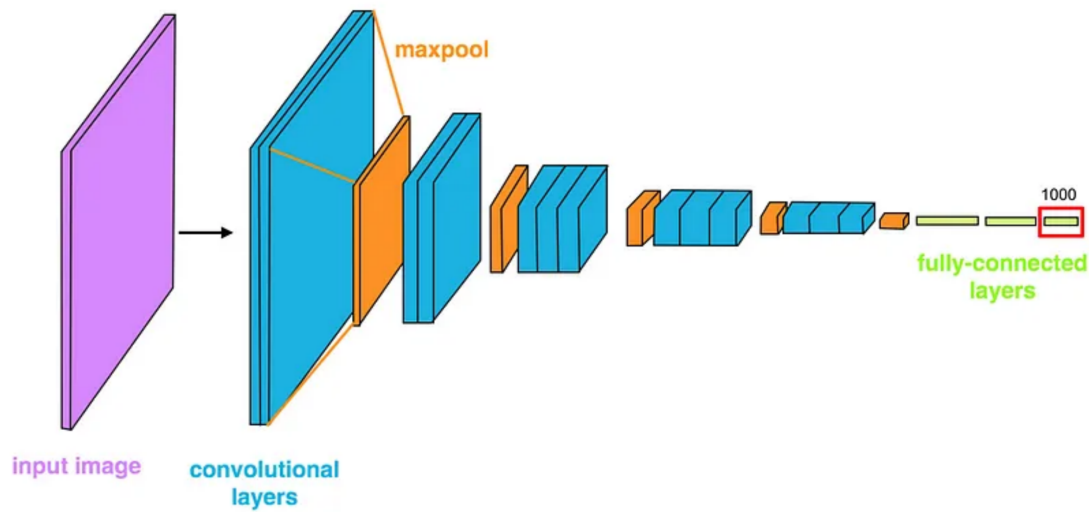


Figure 1.7: VGG 16 Architecture

genetic data, capturing both structural and functional changes in the brain, as well as clinical aspects of AD. Alsubaie et al. (2024).

- **Generative Models:** Generative models such as Generative Adversarial Networks (GANs) Goodfellow et al. (2014) and Variational Autoencoders (VAEs) Kingma & Welling (2013) are networks that aim to generate synthetic data that resemble the characteristics and distribution of input data. They are mainly used in AD research for data augmentation and handling missing data, Sampath et al. (2023), S. Saravanakumar (2022), Bai et al. (2022).

1.4.3 VGG Architecture

The Visual Geometry Group (VGG) architecture, developed by Simonyan & Zisserman (2015), is a CNN-based model known for its depth and straightforward design. It has two variants, VGG16 and VGG19, comprising 16 and 19 layers, respectively. A notable feature of VGG is its use of 3×3 convolution kernels, the smallest size for capturing the basic directions of top, bottom, left, and right. This was a significant deviation from the larger kernels (e.g., 5×5 , 11×11) commonly used at the time. The VGG models were trained for several weeks on a subset of the ImageNet dataset Deng et al. (2009), containing 1.2 million images, for the 2014 ImageNet Large Scale Visual Recognition Challenge (ILSVRC) Russakovsky et al. (2015). VGG achieved a top accuracy of 92.7% in the classification+localization task. The authors have made VGG16 and VGG19 publicly available, and these models are now accessible as pre-trained models in deep learning frameworks like TensorFlow and PyTorch. VGG's high image recognition capabilities have made it widely used in Alzheimer's Disease (AD) research for early detection and classification of different AD stages, as demonstrated by its performance on ImageNet Hon & Khan (2017), Helaly et al. (2021).

Chapter 2

State Of The Art

2.1 Introduction

As the research in machine learning and deep learning techniques progresses, these methods are being increasingly utilized in order to optimize processes and tackle challenges across various domains including medical and healthcare sectors. This chapter contains a review of significant contributions in machine learning and deep learning methods for detection and classification of AD. These contributions span a diverse selection of algorithms and methods, and utilize varying modalities and data sources. To summarize these contributions, we included recapitulating tables that describe the method, data source, modalities, classification type, classification targets, and results.

2.2 Classic Approaches

Chaves et al. (2013) utilized method that integrates discretization and association rule (AR)-based classification for early Alzheimer's disease (AD) detection. The problem addressed is the need for early diagnosis using neuroimaging data, particularly Single Photon Emission Computed Tomography (SPECT) and Positron Emission Tomography (PET). The SPECT database used included imaging studies from subjects referred by neurologists at the Virgen de las Nieves hospital in Granada, Spain. While the PET data was sourced from the ADNI database. The proposed Computer Aided Diagnosis (CAD) system uses intensity-based discretization of 3D voxel features to select regions of interest (ROIs). AR mining is then applied to identify relationships among brain areas in control subjects, with a focus on identifying distinctive patterns for AD. The system achieved high accuracy, with 96.91% for SPECT and 92% for PET. Metrics like sensitivity (up to 94.64% for SPECT) and specificity (up to 100%) underscore the system's effectiveness.

2.3 Machine Learning-based Approaches

2.3.1 Bayesian Classifier

Bayesian classifiers represent uncomplicated probabilistic classification models that assume feature independence. Grounded in Bayes' theorem, these classifiers produce a classification as a probability based on the input features Shanthamallu et al. (2017).

López et al. (2009) proposed a Computer-Aided Diagnosis (CAD) system for the diagnosis of AD based on multivariate approaches such as Principal Component Analysis (PCA) and Linear Discriminant Analysis (LDA). These techniques were utilized to reduce high dimensionality and extract relevant features from the used SPECT and PET datasets, which were obtained from the "Virgen de las Nieves" Hospital in Granada, Spain, and the "Clinica PET Cartuja" in Seville, Spain, respectively. Both datasets contained labeled normal control and AD cases. A Bayesian classifier was used for the classification task. It was evaluated using Leave-One-Out cross-validation, which yielded accuracy rates of 98.33% and 93.41% for PET and SPECT images, respectively.

Seixas et al. (2014) proposed a Bayesian Network (BN) decision model for supporting the diagnosis of dementia, Alzheimer's disease (AD), and Mild Cognitive Impairment (MCI). The BN model was built using a combination of expert knowledge and data-oriented modeling. The structure of the network is based on current diagnostic criteria and input from domain experts. The parameters of the network were estimated using a supervised learning algorithm from a dataset of real clinical cases, which consists of patients and normal controls from two institutions: CERAD (Consortium to Establish a Registry for Alzheimer's Disease) and CAD (Center for Alzheimer's Disease and Related Disorders). The dataset includes attributes such as neuropsychological test results, patient demographic data, symptoms, and signs. The proposed BN network scored an F1 score of 0.65 on the CERAD dataset and 0.82 on the CAD dataset in AD diagnosis. Limitations of the study include the use of a limited dataset and the absence of certain relevant neuropsychological tests in the dataset.

2.3.2 Support Vector Machines

Support Vector Machine (SVM) is a machine learning algorithm that was first introduced in the 1990s by Vladimir N. Vapnik and his colleagues and used for both regression and classification problems. Most previous biomarker studies focused on one specific biomarker or compared the sensitivity and specificity of different single biomarkers. Some researchers have proposed that multi-view neuroimaging biomarkers can get better performance than single-view in the detection of AD, as demonstrated by the study of (Hinrichs et al. (2009), Zhang et al. (2011)) which found that using inter-cluster biomarker always get the best result.

Dukart et al. (2013) suggested using SVM on combined information from multiple biomarkers to improve the detection and differentiation of AD and frontotemporal lobar degeneration. The methods involved pre-processing and classification algorithms applied to two different datasets: the Cognitive Neurology Clinic at the

University of Leipzig and the Alzheimer’s Disease Neuroimaging Initiative (ADNI) database. The data types used were FDG-PET and MRI scans as well, and the preprocessing algorithm was designed to facilitate the combination of different image modalities. The method achieved an accuracy of 90%, specificity of 87.8%, and sensitivity of 91.8% on both magnetic resonance images and PET. This suggests that machine learning techniques, particularly when combining FDG-PET and MRI data, can achieve high accuracy in Alzheimer’s detection.

Another study (Kruthika et al. (2018)) proposed a method for classifying Alzheimer’s Disease (AD) and Mild Cognitive Impairment (MCI) and Normal Control (NC) on MRI data using volumetric measurements of brain structures relevant to the diagnosis of AD. These measures include the hippocampus, medial temporal lobe, ventricles, amygdala as well as whole brain volume. These measures were extracted from the images using FreeSurfer software ¹. The images were obtained from the Alzheimer’s Disease Neuroimaging Initiative (ADNI) dataset. The volume measurements were then considered as features for the SVM classifier. The authors chose the AUC (Area Under the Curve) as the evaluation metric in this study, claiming that it is less sensitive to differences in the class distribution within the data, which makes it more robust in dealing with skewed data compared to accuracy. The results showed that the hippocampal volume measurement is the best performing feature for AD/NC, AD/MCI, NC/MCI classification scoring an AUC value of 95.75%, 79.13%, and 64.09% respectively.

2.3.3 Logistic Regression

Logistic regression is one of the simplest classification machine learning models. It fits a sigmoid function to the data and outputs probabilistic class predictions for new inputs according to that function. Logistic regression has been used for Alzheimer’s classification in several studies, usually in conjunction with other methods that handle image processing and feature extraction Ruyi Xiao (2021), Johnson et al. (2014).

Ruyi Xiao (2021) proposed a method for the early diagnosis of Alzheimer’s disease using a sparse logistic regression model with the generalized elastic net. The researchers aim to accurately predict individuals at high risk of developing Alzheimer’s disease for future treatment. The high-dimensional small sample characteristics of Alzheimer’s disease data pose challenges for logistic regression, which the elastic net solves by selecting only the most discriminant features. The parameters of the regularization were tuned using ten-fold cross-validation and evaluated using accuracy, sensitivity, and specificity. The proposed model performed better than other methods including SVM, Random Forest, CNN, and RNN trained on 197 subjects from the baseline MRI data of ADNI, achieving an accuracy score of 95.61% for AD vs. HC (healthy controls), 84.67%, for MCI (mild cognitive impairment) vs. HC, and 75.87% for cMCI (converters) vs. sMCI (stable).

Johnson et al. (2014) combined a genetic algorithm (GA) with logistic regression to predict healthy controls (HC) conversion to MCI/AD and MCI to AD after 36 months. The data used in this study is a set of neuropsychological and mood rating scales including the Mini-Mental State Examination (MMSE), Clock Drawing

¹FreeSurfer (harvard.edu)

Test (CDT), and Clinical Dementia Rating scale (CDR) among others, of individuals aged 60 years or older, categorized as either cognitively healthy or meeting clinical criteria for mild cognitive impairment (MCI) or Alzheimer’s disease (AD). This data was obtained from the AIBL study. The genetic algorithm was used to search for the most significant combination of features which were represented using strings of binary values, each combination (population individual) was used for the training of a logistic regression model, of which the AUC score was used as the fitness score. Then, through crossover and mutation, the search space was probed for the fittest combination of features to be considered for the final model. After running the GA 50 times, it selected different combinations of features for predicting progression from HC to MCI/AD that has achieved AUC of 0.90% and progression from MCI to AD with AUC of 0.86%, highlighting the superiority of using combinations of features over individual ones.

2.3.4 K-means

K-means Forgy (1965) is an unsupervised learning technique that is applied to classify unlabeled data points into a specific number of groups or clusters. This is achieved by assigning each data point to the nearest mean. The number of clusters is either defined based on the nature of the data or based on clustering validity measures.

In Escudero et al. (2011), the authors addressed the pressing need for objective means to detect Alzheimer’s disease (AD) early, allowing for targeted interventions and treatment monitoring. The study proposed the creation of a Bioprofile of AD, aiming to reveal key disease patterns in subjects’ biodata. The study utilizes the ADNI database, incorporating modalities such as demographic, clinical, MRI, and CSF data from CN, MCI, and AD subjects. K-means clustering is applied to data features to divide subjects into pathologic and non-pathologic groups in five clinical scenarios. The preliminary results confirm the presence of an important AD pattern in the biodata of controls, AD, and Mild Cognitive Impairment (MCI) patients. Furthermore, the Bioprofile shows potential for early detection of AD at the MCI stage by dividing MCI subjects into groups with different rates of conversion to AD. The results are measured using clustering rates, with statistical significance assessed using the Mann-Whitney U test. The limitations of the study include the need for further validation and the potential impact of variable weighting on the assignment of subjects to the Bioprofile of AD.

Olle Olle et al. (2024) Proposed two approaches for classification of Alzheimer’s disease to CN and AD. the dataset provided from ADNI including 602 MRI images. The Kmeans approach using CNN architecture for training achieved an AUC 0.887, and accuracy of 82.0%. In the second approach, Principal Component Analysis PCA was used in feature reduction while using ANN architecture for training, reporting an AUC of 0.941 and an accuracy of 91.0%.

The study Paul & Hoque (2010) applied the algorithm of k-Means-Mode on the dataset of the University of California at Irvine (UCI) Machine Learning Repository and a diabetes dataset, and reported an accuracy about of 95%. while other algorithms like K-Means and K-Mode showed accuracies lower than 65%. This indicates that the K-Means-Mode is better than others in clustering the data and will

be helpful in data analysis.

2.3.5 Multi-layer Perceptron

Raju et al. (2021) presented a multi-class classification algorithm for the detection of Alzheimer’s disease (AD), Mild Cognitive Impairment (MCI), and Normal Control (NC). The data used in this study was 465 sMRI images, including 132 AD, 181 MCI, and 152 NC images from the ADNI dataset. Each one of these images was partitioned into 27 overlapping patches and fed into a 3D CNN for feature extraction, which then got concatenated into a feature vector. A multi-layer perceptron was then trained on the resulting features. The results indicated an accuracy of 96.66% in the ternary classification task. A heatmap of the main affected brain regions relating to AD and MCI was also generated using Gradient Weighted Class Activation Mapping (Grad-CAM) being the medial temporal lobe’s subcortical structures such as the hippocampus, entorhinal cortex, amygdala, and Para hippocampus, confirming previous research in the field.

Qiu et al. (2020) proposed an interpretable deep learning framework for the classification of AD using multi-modal MRI, age, gender, and Mini-Mental State Examination score data from the ADNI dataset. The framework consists of a fully convolutional network (FCN) trained on MRI patches for each individual. It generates probability maps of AD status for local brain regions and three multilayer perceptron (MLP) models. The first MLP was trained on the probability maps generated by the FCN, the second MLP model was trained on age, gender, and MMSE score, and the third model was trained on combined modalities. The models’ performance was compared against an international group of practicing neurologists on a randomly sampled cohort of ADNI participants having all the modalities (MRI, MMSE score, age, and gender) provided. The performance of the neurologists varied due to different clinical practices. The deep learning model that was trained on only MRI data (MRI model) reached an accuracy of 0.834 ± 0.020 , and outperformed the average neurologist (accuracy: 0.823 ± 0.094). When age, gender, and MMSE information were added to the model, the performance increased significantly (fusion model; accuracy: 0.968 ± 0.014).

2.4 Deep Learning-based Approaches

2.4.1 Transfer Learning (TL) approaches

Aderghal et al. (2018) proposed a cross-modal transfer learning approach. Specifically, from structural MRI to Diffusion Tensor Imaging (DTI) modality, for NC, AD, and MCI classification. Their motivation was the lack of large datasets in both modalities, which led to overfitting. With data obtained from the ADNI database, the authors applied data augmentation to increase the number of samples both for training and validation sets. Then, they pre-trained a set of CNN models on the augmented data, classifying AD vs. NC, NC vs. MCI, and MCI vs. AD on the Sagittal, Axial, and Coronal projections, from which they selected the best, using a majority vote. The model is then fine-tuned on Mean Diffusivity (MD) data extracted from DTI by initializing it with the parameters obtained from the

pre-training. The final model achieved classification accuracies of 92.5% for AD vs. NC, 85.0% for AD vs. MCI, and 80.0% for MCI vs. NC.

In Hon & Khan (2017), the authors applied transfer learning on two proven models, VGG16 and Inception V4 with weights pre-trained on ImageNet to detect AD. The data consists of MRI scans from 100 health controls (HC) and 100 AD subjects from the OASIS dataset. An entropy-based selection mechanism was used to select the most informative 32 slices from the 3D scans, resulting in a total of 6,400 images. After training the models using 5-fold cross-validation, the average accuracy achieved by the fine-tuned VGG16 and Inception V4 models was 92.3% and 96.25%, respectively, which was comparable to the five state-of-the-art methods that the authors included for comparison.

2.4.2 Convolutional Neural Networks

Convolutional Neural Network (CNN) is a type of neural network that is particularly effective in image recognition and classification tasks. CNNs are composed of multiple layers, including convolutional layers and activation layers. These layers work together to extract features and then make predictions based on these features. CNNs are designed to automatically and adaptively learn, but the training process involves feeding a large dataset. In the context of Alzheimer’s disease detection, CNNs can be trained to analyze brain images, such as MRI scans, and identify patterns or abnormalities that are indicative of the disease.

In the study of Ebrahimi et al. (2021), the authors explore the effectiveness of CNNs in detecting Alzheimer’s disease using MRI images, by comparing different CNN architectures including 2D and 3D CNNs. The main contribution of the study is the introduction of transfer learning from a 2D to 3D data set. For this purpose, they proposed two approaches: the first utilizes 2D convolutional neural networks (CNNs) to extract AD-related features from individual image slices, while the second combines 2D CNNs with long short-term memory (LSTM) to capture spatial connections in the 2D image slices. The performance of the proposed approaches is evaluated using the Alzheimer’s Disease Neuroimaging Initiative (ADNI) dataset. The results show that Multi-view ResNet-18 using transfer learning had 84.38% accuracy, and Multi-view SqueezeNet using transfer learning had 90.62% accuracy. The same performance was achieved by SqueezeNet + LSTM. The research highlights training 3D CNNs. In addition, the 3D voxel-based method with transfer learning outperforms the other methods with accuracy 96.88%, sensitivity 100% and specificity 94.12%. This indicates the potential of deep learning models and transfer learning in improving the precision of AD detection using MRI images.

Helaly et al. (2021) proposes a system that includes three fundamental stages: feature extraction, feature reduction, and classification. CNN is used to combine these stages. The other method used is VGG19. The dataset is collected from ADNI and consists of 300 patients divided into four classes: Alzheimer’s disease (AD), early mild cognitive impairment (EMCI), late mild cognitive impairment (LMCI), and normal controls (NC), with a total of 4800 MRI images. The results show that the CNN architectures achieved very promising accuracies, with 93.61% and 95.17% for 2D and 3D multi-class AD stage classifications, respectively. Additionally, the VGG19 pre-trained model achieved a precision of 97%. Under the circumstances

imposed by the Covid-19 pandemic, The authors also established a web service based on the proposed CNN architectures that is aimed to predict the AD stage of MRI scans uploaded by patients and doctors.

2.4.3 Recurrent Neural Networks

Recurrent Neural Network (RNN) is a type of artificial neural network designed to handling the sequential data by preserving a memory of the input, unlike other neural networks. RNNs have revolutionized various fields, like his receiving interest in domain of Alzheimer’s disease.

The study of Wang et al. (2018) confirms effectiveness of RNN architectures, especially Long Short Term Memory (LSTM) RNN model, in solving the problem of predicting Alzheimer’s disease (AD) progression. Dataset used from the National Alzheimer’s Coordinating Center (NACC) includes 5432 patients with probable AD from August 31, 2005, to May 25, 2017. The study focus on training the LSTM RNN model on predicting the progress of AD in next medical visit for any patient. Although, the numbers of different visits and uneven intervals for each patient, the results show that the proposed model can predict the patient’s AD progression for the next visit with achieving an accuracy of 99

In Aqeel et al. (2022), the authors proposed a framework of RNN architecture with LSTM and fully connected layers to predict Alzheimer’s disease (AD). The data included MRI biomarkers for 805 subjects from the ADNI dataset. The proposed model predicts biomarkers of patients after 6, 12, 21 18, 24, and 36 months, specifically targeting two classes: MCI and AD. This framework achieved an accuracy of 88.24%.

2.4.4 Generative Adversarial Networks

GAN stands for Generative Adversarial Network. It is a specific type of deep learning architecture that involves discovering and learning regularities or patterns in input data in such a way that the model can be used to create new examples that can be extracted from the original data set. The fundamental idea behind GANs is to train two neural networks that automatically discover and learn the patterns in input data, known as a generator and a discriminator, which compete against each other in a game-like setting in a kind of adversarial fashion. The generator creates synthetic data samples, such as images or text, while the discriminator evaluates the generated data and compares it with real data without knowing which is the real data. The goal of GANs is to train the generator network to produce realistic and high-quality samples that are indistinguishable from real data, which is useful in augmenting data when they have a lack.

SamPATH et al. (2023) proposed a model called Whale-Optimized Deep Generative Adversarial Network (WODGAN), which uses a generator and a discriminator to detect AD stages based on 3D MRI brain neuroimaging. The discriminator is trained using real images, while the generator creates synthetic images using noise and random selection. The WODGAN model is trained and tested using 3D MRIs from the ADNI dataset, which includes 3 Tesla T1-weighted MRI scans. The paper

also discusses the limitations of existing AD detection systems and the importance of early AD identification. The Whale Optimizer (WO) is used during training to improve network efficiency and lower prediction errors. The results and metrics have shown a high accuracy rate of 99.93% in AD stage recognition, highlighting the effectiveness of the WODGAN model in addressing the limitations of existing AD detection systems.

S. Saravanakumar (2022) presents a novel deep learning framework for the early detection of Alzheimer’s disease by distinguishing between multiple classes (e.g., normal, mild cognitive impairment, and Alzheimer’s disease). The proposed methodology involves several key steps, including noise removal, segmentation using the U-Net model, and feature extraction through a convolutional neural network (CNN). The study focuses on the use of a semi-supervised generative adversarial network (GAN) to automatically detect the presence of Alzheimer’s disease in magnetic resonance imaging (MRI) data. The dataset used in the study is the Alzheimer’s Disease Neuroimaging Initiative (ADNI) dataset, The article mentions the use of 1000 images for evaluation, with 700 images used for training. The proposed model achieved a prediction accuracy of up to 77% (AUC = 0.85) for the transformation of mild cognitive impairment (MCI) to Alzheimer’s disease when using individual data.

Bai et al. (2022) presents a novel approach to Alzheimer’s disease detection using generative adversarial networks (GANs) for brain slice image enhancement. The study proposes a three-round learning strategy based on 3D deep convolutional GANs for Alzheimer’s disease staging, aiming to address the overfitting problem caused by the lack of labeled training samples. The proposed BSGAN-ADD model is evaluated on two real-world datasets, comprises 818 structural MRI (sMRI) samples from the Alzheimer’s Disease Neuroimaging Initiative (ADNI) database and 416 subjects from the Open Access Series of Imaging Studies (OASIS) database. The study results demonstrate that the new feature extraction process used in BSGAN-ADD can extract more representative high-level brain features to achieve a significant diagnosis performance gain compared with several typical methods.

2.4.5 Transformer-Based Approaches

Hoang et al. (2023) propose a Vision Transformers (ViT) architecture for the classification of MCI to AD progression using sMRI data of 598 MCI subjects from the ADNI database. The method achieved 83.27%, 85.07% and 81.48% in terms of accuracy, specificity, and sensitivity. For interpretability of the proposed model, the authors also visualized the most contributing brain regions to the prediction of MCI progression, with the findings including the thalamus, medial frontal, and occipital.

Liu et al. (2023) present Multi-Modal Mixing Transformer (3MT), a disease classification transformer for AD and Cognitively Normal (CN) classification and mild cognitive impairment (MCI) conversion prediction to progressive MCI (pMCI) or stable MCI (sMCI). The proposed network leverages multi-modal data. It uses a Cascaded Modality Transformers architecture with cross-attention to mix 12 different feature types including age, gender, education years, APOE4 genotyping, MMSE score, and MRI from the ADNI database. Missing data scenarios were han-

dled using a modality dropout mechanism, ensuring modality independence and full data utilization. The model achieved an accuracy score of 99.4%, a specificity score of 98.9%, and a sensitivity score of 100% on the AD classification task without missing data while it scored 96.3%, 90.3%, and 97.5% in terms of classification accuracy, specificity, and sensitivity, respectively when tested on missing data from the AIBL database.

Sarraf et al. (2023) proposed an optimized Vision Transformer for AD classification (OViTAD) using fMRI and sMRI data from the ADNI database. The main objective was a multi-class prediction of AD, MCI, and HC while aiming to improve the efficiency of the model by reducing the input dimension and the number of heads in the multi-head attention layer to decrease the complexity and trainable parameters of the network. The average performance of the proposed architecture across three repetitions (random data splits) was $97\% \pm 0.0$ and $99.55\% \pm 0.39$ for the two modalities for the multi-class classification experiments. In terms of interpretability, the last fully connected (FC) layer feature vector was multiplied and then summed with each pixel from fMRI brain slices. They were then normalized to obtain color maps.

2.5 Conclusion

In this chapter, we reviewed a wide selection of machine learning and deep learning methods that have been employed for AD classification, such as Bayesian Classifiers, Support Vector Machines (SVM), Logistic Regression, Genetic Algorithms (GA), K-means clustering, 3D Convolutional Neural Networks (CNN), and Fully Connected Networks (FCN). Each method has demonstrated varying degrees of success based on the data source and methodology employed. Diverse data sources like ADNI, OASIS, and AIBL have been utilized, with ADNI being the most extensively used, possibly due to its diversity in terms of the data modalities it offers, this high interest in ADNI highlights the importance of comprehensive datasets in encouraging research in AD. The modalities were used to capture relevant patterns to AD. In their research, the authors heavily relied on MRI data, possibly, due to its high availability in most of the sources. Furthermore, several deep learning techniques were employed, including Transfer Learning, Convolutional Neural Networks (CNN), Generative Adversarial Networks (GANs), and Vision Transformers (ViT). These techniques showed promising results across both binary and multi-class classification tasks, generally surpassing machine learning methods.

Authors	Method	Dataset	Modality	Classification	Targets	Results
Seixas et al. (2014)	Bayesian Classifier	CERAD + CAD	Neuropsychology test results + demographic data + symptoms + signs	Multi class	Dementia vs. AD vs. MCI	F1 score 0.65 (CERAD data), 0.82 (CAD data)
López et al. (2009)	PCA + Bayesian Classifier	Private hospital data	PET + SPECT images	Binary class	AD vs. Non-AD	Accuracy 98.33% and 93.41%
Dukart et al. (2013)	SVM	ADNI + University of Leipzig	MRI + PET	Binary class	AD vs. Non-AD	Accuracy 90%, specificity 87.8%, sensitivity 91.8%
Kruthika et al. (2018)	SVM	ADNI	MRI	Binary class	AD vs. NC, AD vs. MCI, MCI vs. NC	AUC 95.75% , 79.13% , 64.09%
Ruyi Xiao (2021)	Logistic Regression + Generalized Elastic Net	ADNI	MRI	Binary class	AD vs. HC, MCI vs. HC, cMCI vs. sMCI	Accuracy 95.61% , 84.67% , 75.87%
Johnson et al. (2014)	Genetic Algorithm (GA) + Logistic Regression	AIBL		Binary class	HC vs. MCI, HC vs. AD, MCI vs. AD	AUC 90%, AUC 90%, AUC 86%
Escudero et al. (2011)	Bioprofile K-means	ADNI	Demographic + clinical + MRI + CSF	Binary class	AD vs. Non-AD	
Olle Olle et al. (2024)	Kmeans + CNN	ADNI	MRI	Binary class	AD vs. CN	Accuracy 82%, AUC 88.7%
Olle Olle et al. (2024)	PCA + ANN	ADNI	MRI	Binary class	AD vs. CN	Accuracy 91%, AUC 94.1%
Paul & Hoque (2010)	K-Means-Mode	University of California at Irvine (UCI)				Accuracy 95%
Paul & Hoque (2010)	K-Means-Mode	University of California at Irvine (UCI)				Accuracy lower than 65%
Raju et al. (2021)	3D CNN + MLP	ADNI	sMRI	Binary class	NC vs. MCI vs. AD	Accuracy 96.66%
Qiu et al. (2020)	FCN + MLP	ADNI	MRI + age + gender + MMSE	Binary class	AD vs. NC	Accuracy 83.4% (MRI only), 96.8% (fusion model)

Table 2.1: Recapitulating table of machine learning contributions to AD classification

Authors	Method	Dataset	Modality	Classification	Targets	Results
Aderghal et al. (2018)	Transfer Learning from MRI to DTI	ADNI	MRI + DTI	Multi class	AD vs. NC AD vs. MCI MCI vs. NC	92.5% 85.0% 80.0% (accuracy)
Hon & Khan (2017)	Transfer learning on VGG16	OASIS	MRI	Binary class	AD vs HC	92.3% (accuracy)
Hon & Khan (2017)	Transfer learning on Inception V4	OASIS	MRI	Binary class	AD vs HC	96.25% (accuracy)
Ebrahimi et al. (2021)	CNN: Multi-view ResNet-18 with Transfer learning	ADNI	MRI	Binary class	AD vs HC	84.38% accuracy, 87.5% sensitivity, and 81.25% specificity
Ebrahimi et al. (2021)	CNN: Multi-view SqueezeNet with Transfer learning and SqueezeNet + LSTM	ADNI	MRI	Binary class	AD vs HC	90.62% accuracy, 81.25% sensitivity, 100% specificity
Ebrahimi et al. (2021)	CNN: 3D voxel-based with Transfer learning	ADNI	MRI	Binary class	AD vs HC	96.88% accuracy, 100% sensitivity, 94.12% specificity.
Helaly et al. (2021)	2D CNN	ADNI	MRI	Multi class	AD vs EMCI vs LMCI vs NC	accuracy 93.61%
Helaly et al. (2021)	3D CNN	ADNI	MRI	Multi class	AD vs EMCI vs LMCI vs NC	accuracy 95.17%
Helaly et al. (2021)	Transfer Learning + VGG19	ADNI	MRI	Multi class	AD vs EMCI vs LMCI vs NC	accuracy 97%
Sampath et al. (2023)	Whale Optimized Deep GAN (WODGAN)	ADNI + AIBL + OASIS + MIRIAD	3D MRI	Multi class	AD vs MCI vs SMC vs CN	accuracy 99.93%
S. Saravanakumar (2022)	GAN	ADNI	MRI	Multi class	HC vs MCI vs AD	accuracy 70%
Bai et al. (2022)	GANs + CNN	ADNI + OASIS	sMRI	/	/	/
Hoang et al. (2023)	Vision Transformer (ViT)	ADNI	sMRI	Binary class	MCI vs AD	accuracy 83.27%, specificity 85.07%, sensitivity 81.48%
Liu et al. (2023)	Multi-Modality Mixing Transformer (3MT)	ADNI + AIBL	age, gender, education years, APOE4, MMSE score, and MRI without missing data	Multi class	AD vs CN vs MCI vs to pMCI or sMCI	accuracy 99.4%, specificity 98.9%, sensitivity 100%
Liu et al. (2023)	Multi-Modality Mixing Transformer (3MT)	AIBL	MRI with missing data	Multi class	AD vs CN vs MCI vs to pMCI or sMCI	accuracy 96.3%, specificity 90.3%, sensitivity 97.5%
Sarraf et al. (2023)	Optimized ViT (OVITAD)	ADNI	fMRI + sMRI	Multi class	AD vs HC vs MC	accuracy 97% for fMRI and 99.55% for sMRI

Table 2.2: Recapitulating table of deep learning contributions to AD classification

Chapter 3

Implementation and Experiments

3.1 Introduction

In this work, we investigate the application of transfer learning for the classification of multi-class Alzheimer’s disease MRI images. This approach leverages models pre-trained on similar tasks to develop our models, subsequently fine-tuning them with our specific data. This method enhances the predictive accuracy of our models and reduces training time. We selected the VGG16 and VGG19 variants of the VGG architecture as our base models for transfer learning Simonyan & Zisserman (2015). These architectures are deep convolutional networks consisting of 16 and 19 layers, respectively, noted for their depth and straightforward design. The VGG models gained prominence after winning the ImageNet Large Scale Visual Recognition Challenge (ILSVRC) in 2014 Russakovsky et al. (2015).

3.2 Data

The data used in this work were obtained from the Alzheimer’s Disease Neuroimaging Initiative (ADNI) database ¹. Launched in 2003 as a public-private partnership led by Principal Investigator Michael W. Weiner, MD, ADNI aims to determine whether serial magnetic resonance imaging (MRI), positron emission tomography (PET), other biological markers, and clinical and neuropsychological assessments can be combined to measure the progression of mild cognitive impairment (MCI) and early Alzheimer’s disease (AD) ². Specifically, we utilized the ADNI1: Complete 3Yr 3T and ADNI1: Complete 3Yr 1.5T standardized MRI datasets Wyman et al. (2013). These datasets include scans that have undergone preprocessing steps such as gradient inhomogeneity correction (Gradwarp) and B1 correction. The subjects in the 3-year set include individuals with scans taken at screening at 6 months, 1 year, 18 months (MCI only), 2 years, and 3 years (normal and MCI only). We selected this dataset to expose our models to diverse data, allowing them to learn the different changes in the brain over three years for the three classes: cognitively normal (CN), AD, and MCI.

¹Official website: adni.loni.usc.edu

²For up-to-date information, see www.adni-info.org

3.3 Preprocessing

The 3D scans we obtained required a preprocessing pipeline to convert them into 2D slices suitable for training. This pipeline begins with a preselection phase to filter out duplicate scans. Duplicates are identified based on having the same subject ID and date, and those with fewer standardization steps are discarded. Additionally, only MPRAGE scans are retained to maintain data consistency. After this phase, the data remained imbalanced across the subject groups (AD, CN, and MCI). To address this imbalance, we employed two strategies: down-sampling and up-sampling. In the down-sampling approach, we aligned the scan count to the class with the fewest scans, which was AD with 135 scans. The other classes were down-sampled to 135 scans each. To minimize the loss of scan diversity at the subject level, we prioritized selecting subjects with more visits, ensuring greater scan diversity per subject. In the up-sampling approach, we matched the scan count to the class with the most scans, which was MCI with 248 scans. The other classes were up-sampled to 248 scans each by randomly selecting and repeating scans from these classes. This process resulted in two datasets: a down-sampled dataset and an up-sampled dataset, to be used in the training experiments.

The selected scans are forwarded into the main preprocessing step. In this phase, the scans go through four processing steps:

1. **Reorientation.** The scans were reoriented by applying 90, 180, or 270-degree rotations on the different axes as necessary to match the orientation of a standard template image.
2. **Cropping.** As the scans comprise the whole head and neck, it was necessary to crop them to contain only the upper head.
3. **Brain Extraction.** Skull-stripping and extracting only brain tissues and omitting any non-brain tissues helps in retaining only the relevant parts of Alzheimer’s disease.
4. **Atlas Affine Registration.** Due to variations in brain size and dimensions among subjects, as well as potential inconsistencies in repeated scans of the same subject. Registration of the scans to a reference template is essential. This alignment ensures that every voxel consistently corresponds to the same anatomical location in the brain across all scans.
5. **Intensity Normalization.** The intensity values of the scans were rescaled to the range $[-1, 1]$ to facilitate training. This normalization ensures that the pixel values remain within a smaller numerical range, which is beneficial for neural network-based models during the training.
6. **Central Slice Cropping.** From each scan, only 30 slices were taken from the center along the z-axis in an effort to balance capturing the most relevant information to the diagnosis of AD and reducing computational costs.

This pipeline produces 30 2D images (slices) per scan, resulting in a total of 12,150 images (4,050 images per class) in the down-sampled dataset and 22,320 images in the up-sampled dataset (7,440 images per class). Most of the steps in this phase were executed using the FSL Neuroimaging tool. The implementation of this pipeline is available here.

3.4 Experiments

In the context of training deep learning (DL) models, transfer learning plays a remarkable role in enhancing performance and efficiency by leveraging knowledge gained from one domain to improve performance in a different but related task.

The experimentation setup includes two convolutional neural network models, each utilizing a pre-trained VGG architecture (VGG16 and VGG19) as the base model. Both models are trained on the up-sampled and down-sampled datasets described earlier, resulting in four experiments. The pre-trained models act as feature extractors, capturing intricate patterns from the input images. The VGG16 and VGG19 models were originally trained on the ImageNet dataset, which contains over 1.4 million images across 1,000 different classes.

3.4.1 Architecture

The proposed models use VGG16 and VGG19 as the base architectures. The VGG16 architecture comprises 13 convolutional layers and 3 fully connected layers, while the VGG19 architecture includes 16 convolutional layers and 3 fully connected layers. We adjusted the dimensions of the input images to be compatible with the dataset. Both models use weights pre-trained on the ImageNet dataset and exclude the top (fully connected) layers. To retain the learned features and prevent them from being updated during training, all layers of the base model were frozen, allowing weight updates only on the top model, which has the following architecture:

- **Flatten Layer:** Converts the 3D output from previous layer into a 1D vector.
- **Dense Layer:** A fully connected layer with 256 units and ReLU activation.
- **Dense Layer:** Another fully connected layer with 128 units and ReLU activation
- **Output Layer:** The last Dense layer with 3 units, using softmax activation for classification.
- **Batch Normalization** layers are added after each fully connected (Dense) layer. Batch normalization helps stabilize the training process and improves model performance.
- **Dropout** layers are added after each fully connected layer with a dropout rate of 0.5 to reduce overfitting.

3.4.2 Metrics Used in Evaluation

To thoroughly evaluate the performance of our models, we used various metrics that provide a comprehensive view of model effectiveness. These metrics include accuracy, precision, recall, F1-score, and the receiver operating characteristic curve (ROC) as well as the area under the receiver operating characteristic curve (AUC ROC).

- **Accuracy** is the proportion of correctly predicted instances out of the total instances. It is a simple yet effective measure of overall model performance.

$$\mathbf{Accuracy} = \frac{\text{True Positives} + \text{True Negatives}}{\text{Total Number of Predictions}}$$

- **Loss** quantifies the difference between the predicted values and the actual values. In classification tasks, loss is typically measured using cross-entropy loss, which provides a measure of how well the predicted probabilities match the actual class labels.
- **Precision** measures the accuracy of the positive predictions. It is the ratio of true positive predictions to the sum of true positive and false positive predictions.

$$\mathbf{Precision} = \frac{\text{True Positives}}{\text{True Positives} + \text{False Positives}}$$

- **Recall** assesses the model's ability to identify all relevant instances. It is the ratio of true positive predictions to the sum of true positives and false negatives.

$$\mathbf{Recall} = \frac{\text{True Positives}}{\text{True Positives} + \text{False Negatives}}$$

- **F1-Score** is the harmonic mean of precision and recall, providing a single metric that balances both concerns. It is particularly useful when dealing with imbalanced datasets.

$$\mathbf{F1-score} = 2 \times \frac{\text{Precision} \times \text{Recall}}{\text{Precision} + \text{Recall}}$$

- **ROC AUC** is the area under the receiver operating characteristic curve (ROC AUC) that measures the model's ability to distinguish between classes. It provides an aggregate measure of performance across all classification thresholds.

$$\text{ROC AUC} = \int_0^1 \text{TPR}(t) d\text{FPR}(t)$$

3.4.3 Experimental results

In this section, we present a comprehensive evaluation of the models across the four experiments mentioned above. By assessing these models on differently sampled datasets, we aim to highlight the impact of data sampling techniques and pre-trained models on model accuracy, generalization, and training stability. Our analysis provides insights into how these architectures perform under varying data conditions and demonstrates the robustness and adaptability of transfer learning in enhancing Alzheimer's disease detection.

3.4.3.1 Training on down-sampled data

VGG16 was trained with a batch size of 64 and a learning rate of 0.001 for 100 epochs. The validation loss closely followed the training loss, showing a downward trend with occasional fluctuations but stabilizing at the end, as shown in Figure 3.1. The model achieved an overall accuracy of 99.18% and F1-scores of 99.13%, 99.39%, and 99.01% for the AD, CN, and MCI classes, respectively. Although the model showed slightly higher error rates in detecting the AD class (as indicated by recall), it achieved the best precision among all classes, as illustrated in Figure 3.2. Table 3.1 gives more details on the testing performance for each class.

	Precision	Recall	F1-score	Support
MCI	0.9889	0.9914	0.9901	810
AD	0.9975	0.9852	0.9913	810
CN	0.9890	0.9988	0.9939	810
macro avg	0.9918	0.9918	0.9918	2430

Table 3.1: Classification Report of VGG16 trained on down-sampled data

VGG19 was trained with a batch size of 32 and a learning rate of 0.001 for 100 epochs. The learning curve exhibited occasional fluctuations but demonstrated more stability towards the end, as shown in Figure 3.4. The model achieved a high accuracy of 99.59%, with an F1-score of 99.57% for AD and CN, and 99.63% for MCI. It showed a lower error rate in detecting the CN class compared to the AD class while maintaining high precision in all three classes. The classification report in Table 3.2 and confusion matrix in Figure 3.5 provide more details of the model’s testing performances.

3.4.3.2 Training on up-sampled data

Next, we examine the results of our VGG16 and VGG19 models after training and testing on the up-sampled dataset. This analysis enables us to understand the impact of increased data quantity on the models’ accuracy and generalization abilities.

With this dataset, VGG16 was trained for 100 epochs with the default batch size and learning rate. Both training and validation losses show a downward trend with occasional fluctuations, which decrease in range over the epochs as shown in Figure 3.7. As detailed in Table 3.3, the model achieved an accuracy of 98.49%, with an F1-score of 99%, 98.35% and 98.15% for AD, CN and MCI, respectively. The precision is nearly equal in all classes, as illustrated in Figure 3.8.

	Precision	Recall	F1-score	Support
MCI	0.9975	0.9951	0.9963	810
AD	0.9963	0.9951	0.9957	810
CN	0.9938	0.9975	0.9957	810
macro avg	0.9959	0.9959	0.9959	2430

Table 3.2: Classification Report of VGG19 trained on down-sampled data

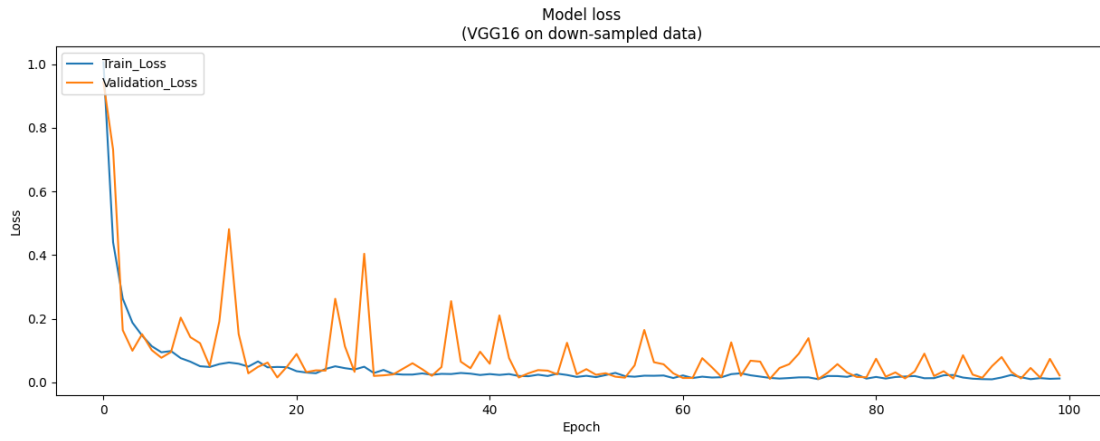


Figure 3.1: Training and validation loss of VGG16 trained on down-sampled data

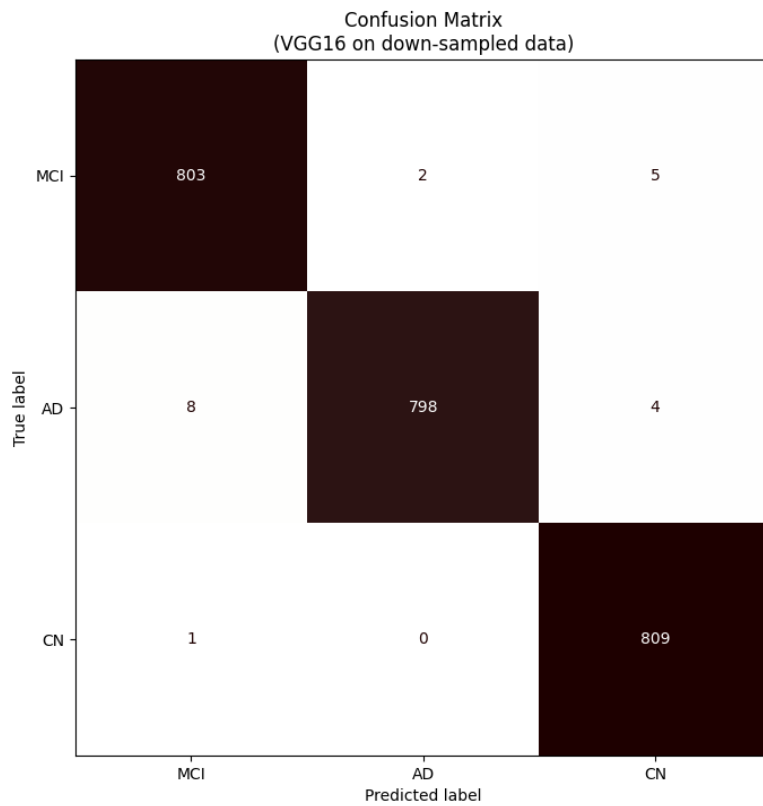


Figure 3.2: Confusion matrix of VGG16 trained on down-sampled data

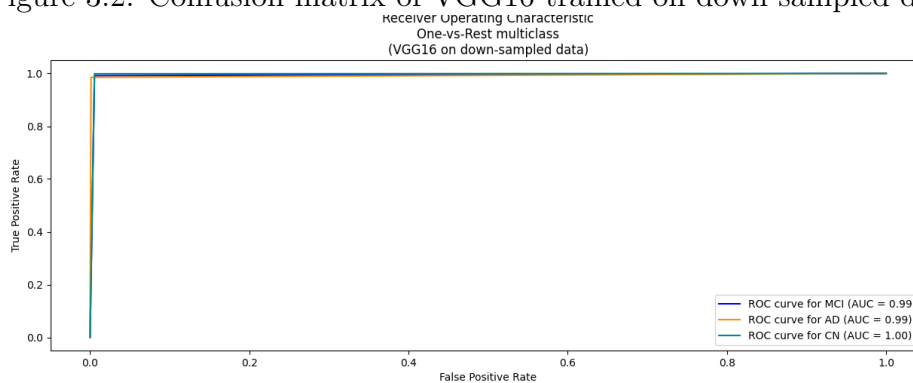


Figure 3.3: Receiver Operating Characteristic curve of VGG16 trained on down-sampled data



Figure 3.4: Training and validation loss of VGG19 trained on down-sampled data

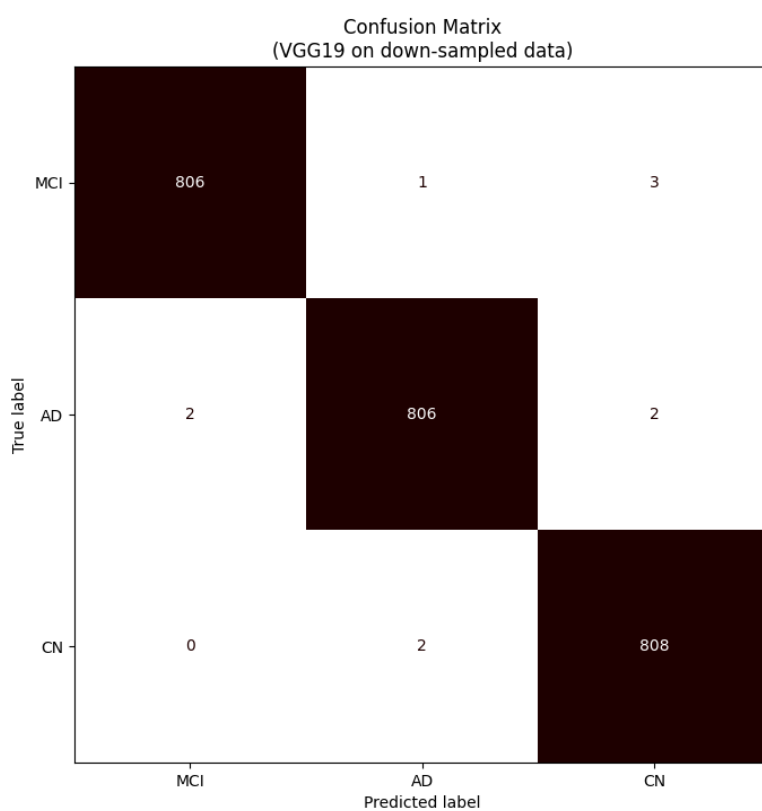


Figure 3.5: Confusion matrix of VGG19 trained on down-sampled data

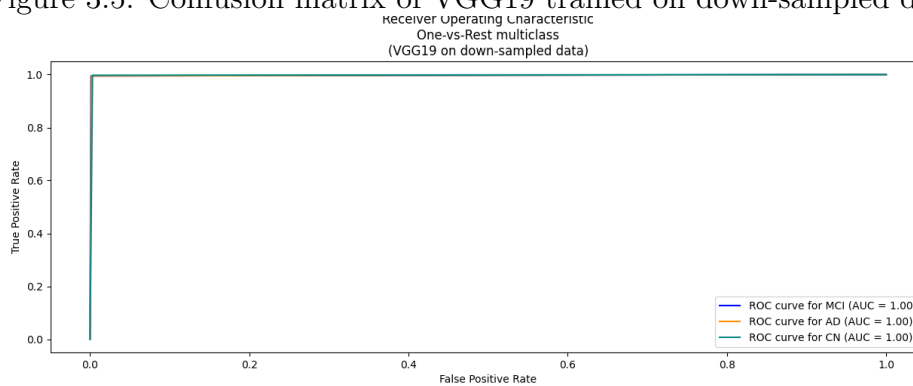


Figure 3.6: Receiver Operating Characteristic curve of VGG19 trained on down-sampled data

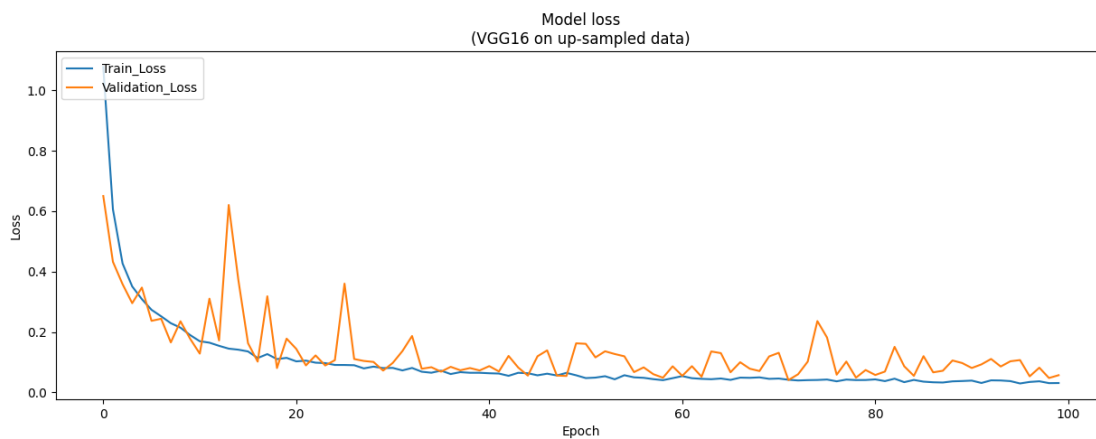


Figure 3.7: Training and validation loss of VGG16 model trained on up-sampled data

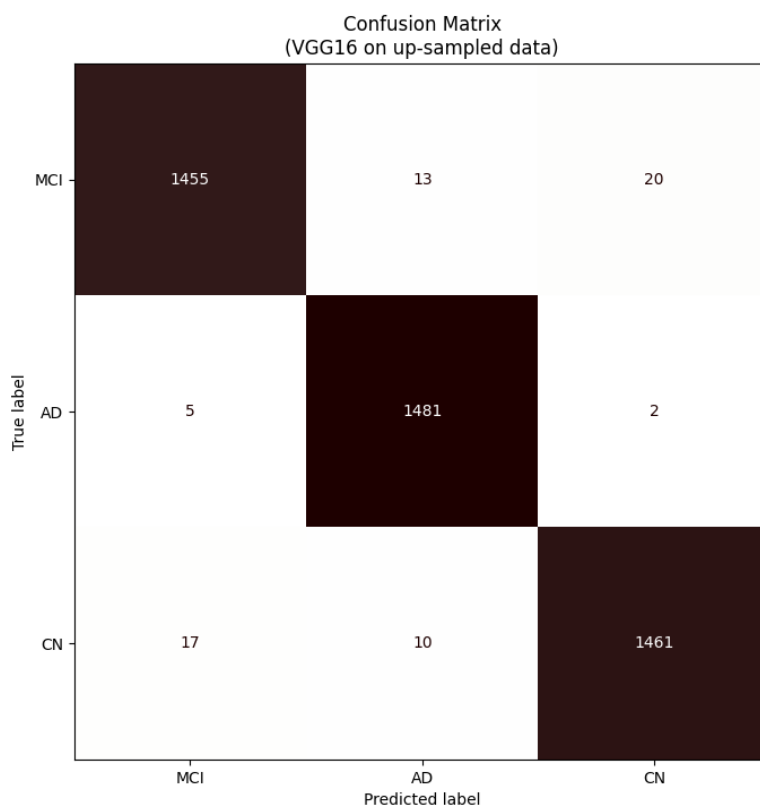


Figure 3.8: Confusion Matrix of VGG16 on up-sampled data

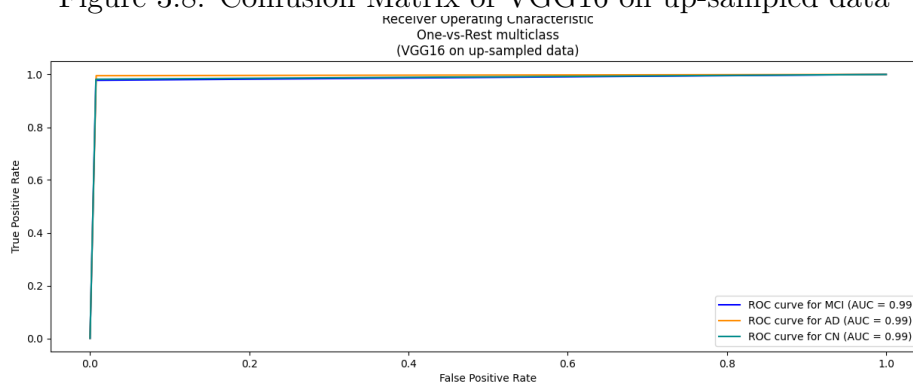


Figure 3.9: Receiver Operating Characteristic curve of VGG16 trained on up-sampled data

	Precision	Recall	F1-score	Support
MCI	0.9851	0.9778	0.9815	1488
AD	0.9847	0.9953	0.9900	1488
CN	0.9852	0.9819	0.9835	1488
macro avg	0.9850	0.9850	0.9850	4464

Table 3.3: Classification Report of VGG16 trained on up-sampled data

For VGG19, the batch size was set to 32 with a default learning rate of 0.001, the training was carried out for 100 epochs. Despite some fluctuations, the validation loss generally improved and stabilized towards the later epochs, as shown in Figure 3.10. The model achieved an accuracy score of **98.14%**, and an F1-score of **98.7%**, **97.56%**, and **98.15%** in AD, CN, and MCI, respectively. The model’s highest error was misclassifying CN images as AD and MCI, resulting in a low CN recall of **95.50%**. However, the AD class achieved a high recall of **99.32%**, as shown in Figure 3.11. More details regarding the testing performance for each class are provided in Table 3.4.

	Precision	Recall	F1-score	Support
MCI	0.9674	0.9960	0.9815	1488
AD	0.9808	0.9933	0.9870	1488
CN	0.9972	0.9550	0.9756	1488
macro avg	0.9818	0.9814	0.9814	4464

Table 3.4: Classification Report of VGG19 trained on up-sampled data

3.4.4 Discussion

When reviewing the performance of the models trained so far, namely, VGG16 and VGG19 architectures on the down-sampled and up-sampled datasets, we observe that all the models performed reasonably well. However, as shown in Table 3.5 and Figure 3.13, the VGG19 model trained on down-sampled data stands out as the most promising in terms of accuracy, AUC ROC, average precision, recall, and F1-score over the classes. The VGG16 model trained on down-sampled data follows closely behind, indicating an advantage for models trained on down-sampled data over those trained on up-sampled data. However, Figure 3.14 shows that models trained on up-sampled data perform better in some instances. For example, the VGG16 and VGG19 models trained on up-sampled data exhibit higher AD recall rates (**99.53%** and **99.33%**, respectively) compared to **98.52%** and **99.51%** achieved by the same models trained on down-sampled data. Since detecting all AD subjects is crucial, AD recall is a particularly important metric. Additionally, the VGG19 trained on up-sampled data achieved the highest MCI recall (**99.6%**) despite having the worst CN recall (**95.5%**). This indicates that models trained on up-sampled data tend to have inconsistent classification performance overall.

Table 3.6 shows a comparison of various Transfer Learning (TL) approaches for classifying AD used in recent studies, including our proposed approach, highlighting the performance of pre-trained models. The comparison include Models such

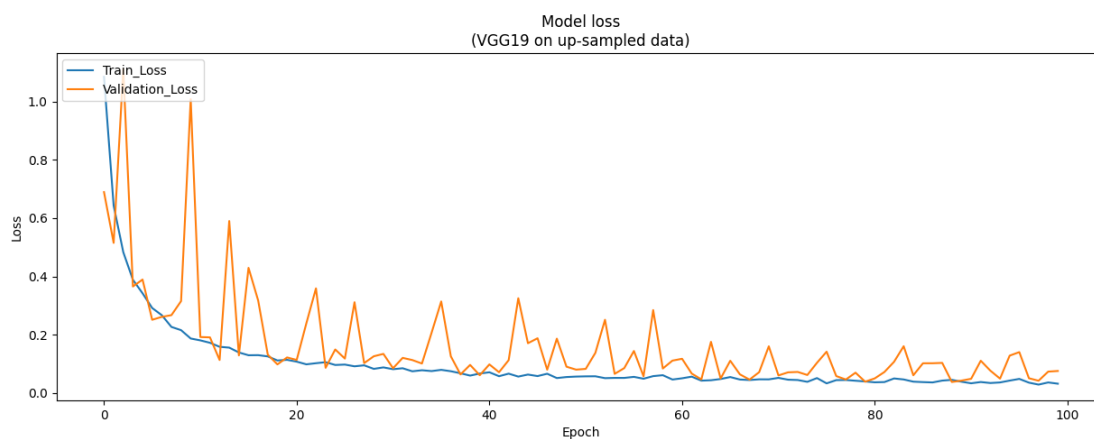


Figure 3.10: Training and validation loss of VGG19 trained on up-sampled data

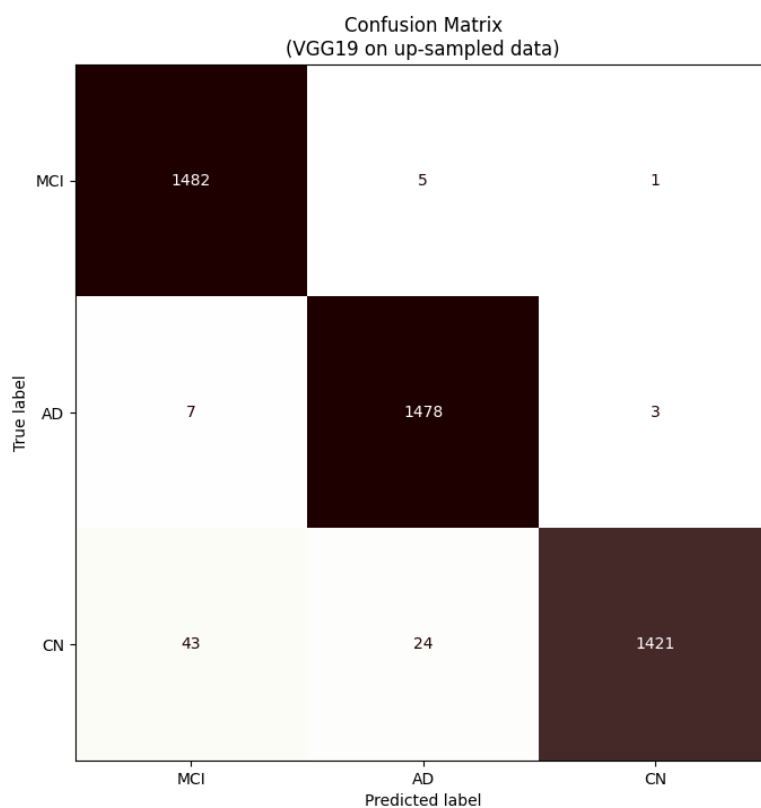


Figure 3.11: Confusion matrix of VGG19 trained on up-sampled data

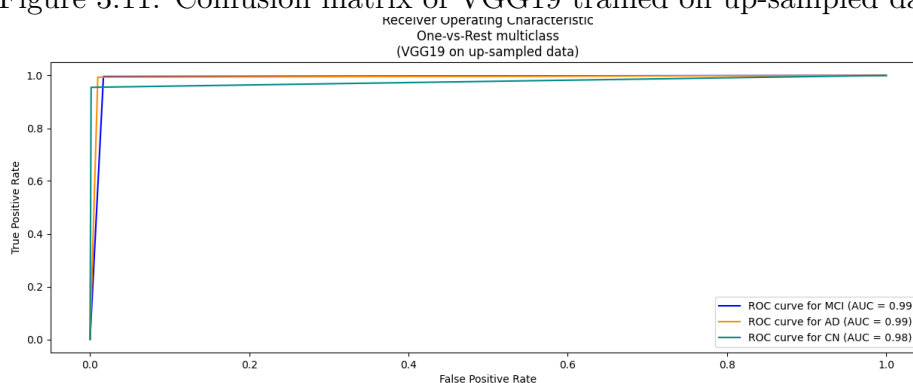


Figure 3.12: Receiver Operating Characteristic curve of VGG19 trained on up-sampled data

Data	Model	Metrics					
		Accuracy	Precision	Recall	F1-score	AUC ROC	Support
down-sampled	VGG16	0.9918	0.9918	0.9918	0.9918	0.9938	2430
	VGG19	0.9959	0.9959	0.9959	0.9959	0.9969	2430
up-sampled	VGG16	0.9850	0.9850	0.9850	0.9850	0.9887	4464
	VGG19	0.9814	0.9818	0.9814	0.9814	0.9861	4464

Table 3.5: Model Performance Summary.

as VGG, Densenet, SqueezeNet, and other, were evaluated using different datasets and images modalities, with classifications task being either binary or multi-class. The metrics used in evaluation is accuracy and Area Under the Curve (AUC). By looking at the table, we can see the accuracy ranging from 69% to 99%, where our approach showed higher accuracy of (98% to 99%). When comparing between the pre-trained models VGG16 and VGG19 that trained with different datasets, we observe that VGG16 and VGG19 of the previous study achieved an Accuracies of 93.75%, 95.35% respectively, while in our approach VGG16 achieved accuracy of 99.18%, and VGG19 has achieved 99.59% with down-sampled data, which outperform other models.

TL-Approaches	Modality	Classification	Accuracy	AUC ROC
VGG-19	PET+MRI (ADNI)	Multi-class (3)	95.35%	None
3D-ResNet	MRI (ADNI)	Binary	79.40%	86.3%
CNN	SMRI, DTI (ADNI)	Binary	96.70%	None
AlexNet	fMRI (OASIS)	Multi-class (5)	94.97%	95%
DenseNet	CT	Multi-class (3)	87.36%	None
SqueezeNet	MRI (OASIS)	Multi-class (4)	82.53%	None
VGG-19	MRI (Kaggle)	Multi-class (4)	77.60%	81%
CNN+ResNet-18	MRI (ADNI)	Multi-class (3)	69.10%	None
ResNet101	MRI (ADNI, OASIS)	Multi-class (4)	93.33%	93%
Efficient Net Model	MRI (ADNI)	Binary	91.36%	83%
Custom-CNN	MRI	Binary	94.7%	None
MobileNet	MRI (ADNI+OASIS)	Multi-class (4)	83.97%	None
CNN+SVM	MRI (OASIS)	Binary	94.44%	None
VGG16	SMRI+FDG-PET	Multi-class (3)	93.75%	None
DenseNet121	MRI (Kaggle)	Multi-class (3)	92.48%	96%
DenseNet169	MRI (Kaggle)	Multi-class (3)	93.00%	97%
DenseNet201	MRI (Kaggle)	Multi-class (3)	96.05%	99%
Proposed				
VGG-16	MRI (ADNI) (down-sampled data)	Multi-class (3)	99.18%	99.38%
VGG-19			99.59%	99.69%
VGG-16	MRI (ADNI) (up-sampled data)	Multi-class (3)	98.50%	98.87%
VGG-19			98.14%	98.61%

Table 3.6: Comparison of the recent studies with proposed approach

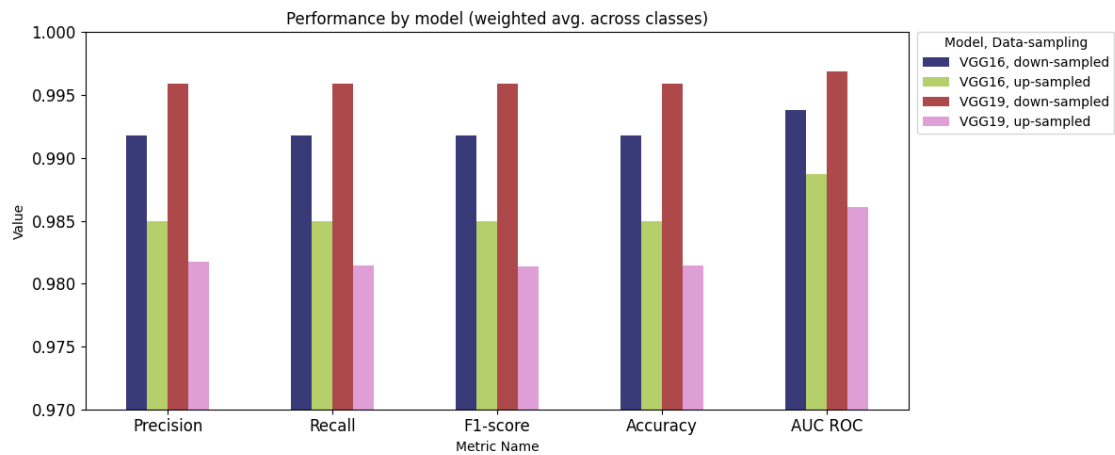


Figure 3.13: Comparison of models performance across all metrics

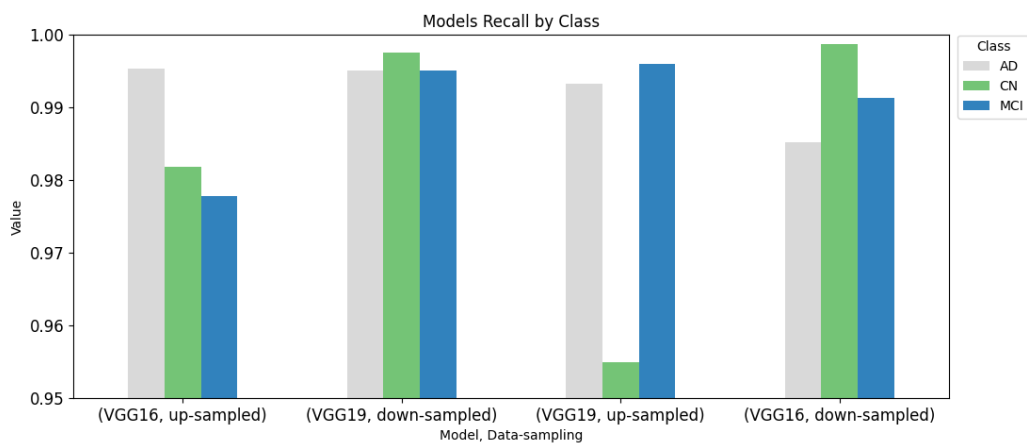


Figure 3.14: Comparison of model's recall by class.

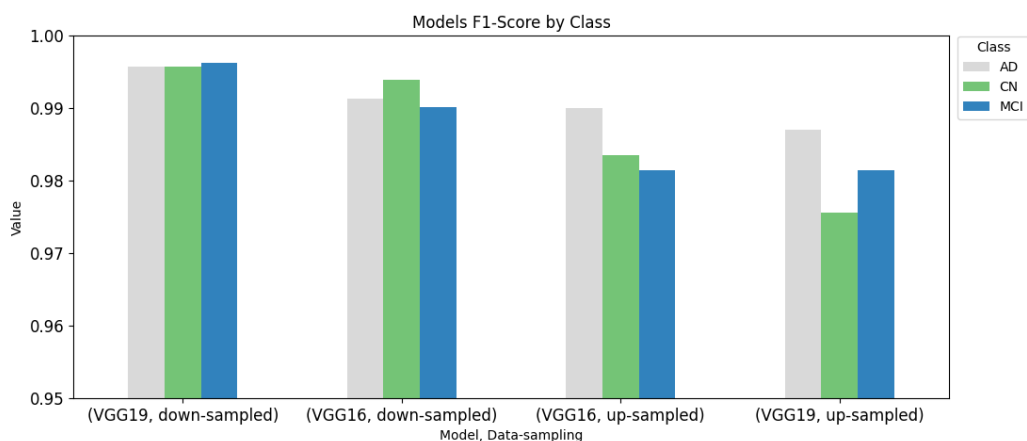


Figure 3.15: Comparison of models F1-score by class

3.5 Conclusion

We have applied transfer learning on multi-class MRI image classification task, by employing VGG16 and VGG19 models pre-trained on ImageNet and training them on two datasets sampled from ADNI to address class imbalance, a down-sampled and an up-sampled dataset, The results indicate that the models performed

generally well in distinguishing between CN, MCI, and AD. with the models trained on down-sampled data having a slight edge in performance over those trained on up-sampled data. Although, we can observe that models trained on up-sampled data achieve better AD recall rates. This might be related to the fact that in the up-sampled dataset, the class with the most repeated scans is AD, which makes the models trained on this data more likely to predict AD than other classes.

Conclusion and Perspectives

Diagnosing Alzheimer’s Disease (AD) involves a lengthy process of neurocognitive tests and interviews to identify the patterns associated with the disease, which are also similar to other conditions, requiring a high level of accuracy. Additionally, the lack of symptoms in the initial stages makes early detection of AD both challenging and crucial for slowing down its progression. In this work, we employed transfer learning to perform multi-class classification on MRI images by leveraging the VGG models and training them on two datasets sampled from ADNI. The results demonstrate the efficacy of this approach in distinguishing between healthy, MCI, and AD subjects, achieving up to 99.59% accuracy. These findings highlight the potential of transfer learning to advance AD research and broaden our understanding of this disease, ultimately improving the quality of life for affected individuals and their caregivers. While this work primarily utilized the VGG architecture and ADNI data, focus on these specific resources allowed for a detailed and controlled investigation. Although other pre-trained models and data sources were not explored, the approach laid a strong foundation for future research. Additionally, while the data augmentation was limited to up-sampling the ADNI data, exploring other augmentation methods may lead to even better results and further validate the robustness of our approach.

Future work should experiment with additional pre-trained models to compare their performance and incorporate different data sources to curate diverse training datasets and to cover the disease progression more comprehensively. It should also employ data augmentation techniques to enrich the training data and enhance model robustness. Additionally, hyperparameter tuning and optimization techniques, such as Grid Search and Bayesian Optimization, could be applied to improve accuracy. Also, using an external dataset when validating the model’s performance will provide a better indication of the model’s robustness, making the models more suitable for deployment in clinical settings. These models could, potentially, become part of a larger system, where they can assist practicing physicians with predictive diagnostics.

Bibliography

- Aderghal, K., Khvostikov, A., Krylov, A., Benois-Pineau, J., Afdel, K., & Catheline, G. (2018, June). Classification of alzheimer disease on imaging modalities with deep cnns using cross-modal transfer learning. In *2018 ieee 31st international symposium on computer-based medical systems (cbms)* (p. 345-350). doi: 10.1109/CBMS.2018.00067
- Alsubaie, M. G., Luo, S., & Shaukat, K. (2024). Alzheimer's disease detection using deep learning on neuroimaging: A systematic review. *Machine Learning and Knowledge Extraction*, *6*(1), 464–505. Retrieved from <https://www.mdpi.com/2504-4990/6/1/24> doi: 10.3390/make6010024
- Aqeel, A., Hassan, A., Khan, M. A., Rehman, S., Tariq, U., Kadry, S., ... Thinnukool, O. (2022). A long short-term memory biomarker-based prediction framework for alzheimer's disease. *Sensors*, *22*(4). Retrieved from <https://www.mdpi.com/1424-8220/22/4/1475> doi: 10.3390/s22041475
- Bai, T., Du, M., Zhang, L., Ren, L., Ruan, L., Yang, Y., ... Deen, M. J. (2022). A novel alzheimer's disease detection approach using gan-based brain slice image enhancement. *Neurocomputing*, *492*, 353–369. Retrieved from <https://www.sciencedirect.com/science/article/abs/pii/S0925231222003782?via%3Dihub> doi: 10.1016/j.neucom.2022.04.012
- Chaves, R., Ramírez, J., & Górriz, J. M. (2013). Integrating discretization and association rule-based classification for alzheimer's disease diagnosis. *Expert Syst. Appl.*, *40*, 1571-1578. Retrieved from <https://api.semanticscholar.org/CorpusID:34455060>
- Deng, J., Dong, W., Socher, R., Li, L.-J., Li, K., & Fei-Fei, L. (2009). ImageNet: A Large-Scale Hierarchical Image Database. In *Cvpr09*.
- Dubey, A., & Rasool, A. (n.d.). Recent advances and applications of deep learning technique.. Retrieved from <https://api.semanticscholar.org/CorpusID:264401275>
- Dukart, J., Mueller, K., Barthel, H., Villringer, A., Sabri, O., Schroeter, M. L., ... others (2013, November 2012). Meta-analysis based SVM classification enables accurate detection of alzheimer's disease across different clinical centers using FDG-PET and MRI. In (Vol. 212, pp. 230–236). Elsevier. Retrieved from <https://www.sciencedirect.com/science/article/abs/pii/S0925492712000856?via%3Dihub> doi: 10.1016/j.psychresns.2012.04.007
- Ebrahimi, A., Luo, S., & Initiative, A. D. N. (2021). Convolutional neural networks for Alzheimer's disease detection on MRI images. *Journal of Medical Imaging*,

- 8(2), 024503. Retrieved from <https://doi.org/10.1117/1.JMI.8.2.024503>
doi: 10.1117/1.JMI.8.2.024503
- Escudero, J., Zajicek, J. P., & Ifeachor, E. (2011). Early detection and characterization of alzheimer's disease in clinical scenarios using bioprofile concepts and k-means. *Annu Int Conf IEEE Eng Med Biol Soc, 2011*, 6470–6473.
- Forgy, E. W. (1965). Cluster analysis of multivariate data: efficiency versus interpretability of classifications. *biometrics*, *21*, 768–769.
- Goodfellow, I., Pouget-Abadie, J., Mirza, M., Xu, B., Warde-Farley, D., Ozair, S., ... Bengio, Y. (2014, 06). Generative adversarial networks. *Advances in Neural Information Processing Systems*, *3*. doi: 10.1145/3422622
- Helaly, H. A., Badawy, M., & Haikal, A. Y. (2021). Deep learning approach for early detection of alzheimer's disease. *Cognitive computation*, 1–17. doi: <https://doi.org/10.1007/s12559-021-09946-2>
- Hinrichs, C., Singh, V., Xu, G., & Johnson, S. (2009). Mkl for robust multimodality ad classification. In *Medical image computing and computer-assisted intervention—miccai 2009: 12th international conference, london, uk, september 20-24, 2009, proceedings, part ii 12* (pp. 786–794).
- Hoang, G. M., Kim, U.-H., & Kim, J. G. (2023). Vision transformers for the prediction of mild cognitive impairment to alzheimer's disease progression using mid-sagittal smri. *Frontiers in Aging Neuroscience*, *15*. Retrieved from <https://www.frontiersin.org/articles/10.3389/fnagi.2023.1102869> doi: 10.3389/fnagi.2023.1102869
- Hon, M., & Khan, N. M. (2017, Nov). Towards alzheimer's disease classification through transfer learning. In *2017 ieee international conference on bioinformatics and biomedicine (bibm)* (p. 1166-1169). doi: 10.1109/BIBM.2017.8217822
- Jan, B., Farman, H., Khan, M., Imran, M., Islam, I. U., Ahmad, A., ... Jeon, G. (2017). Deep learning in big data analytics: A comparative study. *Comput. Electr. Eng.*, *75*, 275-287. Retrieved from <https://api.semanticscholar.org/CorpusID:67282358>
- Johnson, P., Vandewater, L., Wilson, W., Maruff, P., Savage, G., Graham, P., ... Zhang, P. (2014, December). Genetic algorithm with logistic regression for prediction of progression to alzheimer's disease. *BMC Bioinformatics*, *15*(16), S11.
- Kingma, D. P., & Welling, M. (2013). Auto-encoding variational bayes. *CoRR*, *abs/1312.6114*. Retrieved from <https://api.semanticscholar.org/CorpusID:216078090>
- Kruthika, K. R., Rajeswari, Pai, A., & Maheshappa, H. D. (2018). Classification of alzheimer and mci phenotypes on mri data using svm. In S. M. Thampi, S. Krishnan, J. M. Corchado Rodriguez, S. Das, M. Wozniak, & D. Al-Jumeily (Eds.), *Advances in signal processing and intelligent recognition systems* (pp. 263–275). Cham: Springer International Publishing.

- Kumar, A., Sidhu, J., Goyal, A., & Tsao, J. W. (2023). *Alzheimer disease*. StatPearls Publishing, Treasure Island (FL). Retrieved from <http://europepmc.org/books/NBK499922>
- LeCun, Y., Bengio, Y., & Hinton, G. (2015, May 27). Deep learning. *Nature*, *521*(7553), 436–444. (Publisher Copyright: © 2015 Macmillan Publishers Limited. All rights reserved.) doi: 10.1038/nature14539
- LeCun, Y., Boser, B., Denker, J. S., Henderson, D., Howard, R. E., Hubbard, W., & Jackel, L. D. (1989). Backpropagation applied to handwritten zip code recognition. *Neural Computation*, *1*(4), 541-551. doi: 10.1162/neco.1989.1.4.541
- Liu, L., Liu, S., Zhang, L., To, X. V., Nasrallah, F., & Chandra, S. S. (2023). Cascaded multi-modal mixing transformers for alzheimer’s disease classification with incomplete data. *NeuroImage*, *277*, 120267. Retrieved from <https://www.sciencedirect.com/science/article/pii/S1053811923004184> doi: <https://doi.org/10.1016/j.neuroimage.2023.120267>
- López, M., Ramirez, J., Górriz, J. M., Salas-Gonzalez, D., Alvarez, I., Segovia, F., & Chaves, R. (2009, Oct). Multivariate approaches for alzheimer’s disease diagnosis using bayesian classifiers. In *2009 ieee nuclear science symposium conference record (nss/mic)* (p. 3190-3193). doi: 10.1109/NSSMIC.2009.5401703
- Minsky, M., & Papert, S. (1988, 04). (1969) Marvin Minsky and Seymour Papert, Perceptrons, Cambridge, MA: MIT Press, Introduction, pp. 1-20, and p. 73 (figure 5.1). In *Neurocomputing, Volume 1: Foundations of Research*. The MIT Press. Retrieved from <https://doi.org/10.7551/mitpress/4943.003.0015> doi: 10.7551/mitpress/4943.003.0015
- Nabi, H. A., & Zubeldia, J. M. (2002). Clinical applications of (18)f-fdg in oncology. *Journal of nuclear medicine technology*, *30* 1, 3-9; quiz 10-1. Retrieved from <https://api.semanticscholar.org/CorpusID:2181643>
- Olle Olle, D. G., Zoobo Bisse, J., & Abessolo Alo’o, G. (2024). Application and comparison of k-means and pca based segmentation models for alzheimer disease detection using mri. *Discover Artificial Intelligence*, *4*(1), 1–14.
- Paul, R., & Hoque, A. S. M. L. (2010). Clustering medical data to predict the likelihood of diseases. In *2010 fifth international conference on digital information management (icdim)* (pp. 44–49).
- Qiu, S., Joshi, P. S., Miller, M. I., Xue, C., Zhou, X., Karjadi, C., ... Kollachalama, V. B. (2020, 05). Development and validation of an interpretable deep learning framework for Alzheimer’s disease classification. *Brain*, *143*(6), 1920-1933. Retrieved from <https://doi.org/10.1093/brain/awaa137> doi: 10.1093/brain/awaa137
- Raju, M., Gopi, V. P., & V. S., A. (2021, March). Multi-class classification of alzheimer’s disease using 3dcnn features and multilayer perceptron. In *2021 sixth international conference on wireless communications, signal processing and networking (wisnet)* (p. 368-373). doi: 10.1109/WISNET51692.2021.9419393
- Rumelhart, D. E., Hinton, G. E., & Williams, R. J. (1986). Learning internal representations by error propagation.. Retrieved from <https://api.semanticscholar.org/CorpusID:62245742>

- Russakovsky, O., Deng, J., Su, H., Krause, J., Satheesh, S., Ma, S., ... Fei-Fei, L. (2015). ImageNet Large Scale Visual Recognition Challenge. *International Journal of Computer Vision (IJCV)*, 115(3), 211-252. doi: 10.1007/s11263-015-0816-y
- Ruyi Xiao, H. Q. X. Z. Y. Z. C. Z. X. L., Xinchun Cui. (2021). Early diagnosis model of alzheimer's disease based on sparse logistic regression with the generalized elastic net. *Biomedical Signal Processing and Control*, 66, 102362. Retrieved from <https://www.sciencedirect.com/science/article/pii/S1746809420304705> doi: <https://doi.org/10.1016/j.bspc.2020.102362>
- Sampath, R., Sampath, R., & Baskar, M. (2023, Aug). Whale optimized deep generative adversarial network based alzheimer's stages detection using 3d mri brain neuroimaging. *Journal of Computer Science*, 19(8), 998-1014. Retrieved from <https://thescipub.com/abstract/jcssp.2023.998.1014> doi: 10.3844/jcssp.2023.998.1014
- Sarraf, S., Sarraf, A., DeSouza, D. D., Anderson, J. A. E., Kabia, M., & Initiative, T. A. D. N. (2023). Ovitad: Optimized vision transformer to predict various stages of alzheimer's disease using resting-state fmri and structural mri data. *Brain Sciences*, 13(2). Retrieved from <https://www.mdpi.com/2076-3425/13/2/260> doi: 10.3390/brainsci13020260
- Seixas, F. L., Zadrozny, B., Laks, J., Conci, A., & Muchaluat Saade, D. C. (2014). A bayesian network decision model for supporting the diagnosis of dementia, alzheimer s disease and mild cognitive impairment. *Computers in Biology and Medicine*, 51, 140-158. Retrieved from <https://www.sciencedirect.com/science/article/pii/S0010482514000961> doi: <https://doi.org/10.1016/j.combiomed.2014.04.010>
- Shanthamallu, U. S., Spanias, A., Tepedelenlioglu, C., & Stanley, M. (2017, Aug). A brief survey of machine learning methods and their sensor and iot applications. In *2017 8th international conference on information, intelligence, systems applications (iisa)* (p. 1-8). doi: 10.1109/IISA.2017.8316459
- Simonyan, K., & Zisserman, A. (2015). *Very deep convolutional networks for large-scale image recognition*.
- S. Saravanakumar, T. S. (2022). Early alzheimer's disease detection using semi-supervised gan based on deep learning. , 194-198. doi: 10.1109/VLSIDCS53788.2022.9811458
- Wang, T., Qiu, R. G., & Yu, M. (2018). Predictive modeling of the progression of alzheimer's disease with recurrent neural networks. *Scientific reports*, 8(1), 9161.
- Wyman, B. T., Harvey, D. J., Crawford, K., Bernstein, M. A., Carmichael, O., Cole, P. E., ... others (2013). Standardization of analysis sets for reporting results fromadni mri data. *Alzheimer's & Dementia*, 9(3), 332-337.
- Zhang, D., Wang, Y., Zhou, L., Yuan, H., Shen, D., Initiative, A. D. N., et al. (2011). Multimodal classification of alzheimer's disease and mild cognitive impairment. *Neuroimage*, 55(3), 856-867.

Appendices

Appendix A

Deposit Permission

الجمهورية الجزائرية الديمقراطية الشعبية
République Algérienne Démocratique et Populaire
وزارة التعليم العالي والبحث العلمي
Ministère de l'Enseignement Supérieur Et de La Recherche Scientifique

Faculté des Sciences et de la Technologie
جامعة غرداية
كلية العلوم والتكنولوجيا

Département des Mathématiques et d'Informatique
قسم الرياضيات و الاعلام الآلي
Université de Ghardaïa

Ghardaïa le 21/10/2024

Rapport de correction de mémoire de Master SIEC

Je soussigné M/Mme/Mlle : **Slimane Oulad-Naoui**

Président du jury du mémoire de Master intitulé :

Alzheimer's Disease Detection using Deep Learning Techniques

Après les corrections apportées au rapport, je déclare que les étudiants :

Brahim AISSA & Nacer BENYOUB

Sont autorisés à déposer leur manuscrit au niveau du département.

Fait et délivré pour servir et valoir ce que de droit

رئيس قسم الرياضيات و الاعلام الآلي
الحاج موسى المدين



Signature
Slimane Oulad-Naoui

